Research Square

Preprints are preliminary reports that have not undergone peer review. They should not be considered conclusive, used to inform clinical practice, or referenced by the media as validated information.

Synergistic Nano–Bio–Phytochemical Treatment for Microbial Enrichment, Wastewater Remediation, and Enhanced Hydrogen Yield

Shivangi Dubey
Rajiv Gandhi Institute of Petroleum Technology
Rudraksh Srivastava
Rajiv Gandhi Institute of Petroleum Technology
Harish Hirani
Rajiv Gandhi Institute of Petroleum Technology
Japan Trivedi
University of Alberta
Tushar Sharma
tusharsharma.ism@gmail.com

Rajiv Gandhi Institute of Petroleum Technology

Research Article

Keywords: Nano–bio–phytochemical treatment, ZnO nanofluid, Croton bonplandianum, 16S rRNA sequencing, Wastewater treatment, Green hydrogen production

Posted Date: October 22nd, 2026

DOI: https://doi.org/10.21203/rs.3.rs-10848955/v1

License: This work is licensed under a Creative Commons Attribution 4.0 International License. Read Full License

---

Research Article

Synergistic Nano–Bio–Phytochemical Treatment for Microbial Enrichment, Wastewater Remediation, and Enhanced Hydrogen Yield

Shivangi Dubey[b], Rudraksh Srivastava[a], Harish Hirani[b], Japan Trivedi[c], Tushar Sharma[a,*]

[a]EOR-CUS Research Laboratory, Department of Petroleum Engineering & Geoengineering, Rajiv Gandhi Institute of Petroleum Technology Jais, Amethi, Uttar Pradesh-229304, India.

[b]Department of Mechanical Engineering, Rajiv Gandhi Institute of Petroleum Technology Jais, Amethi, Uttar Pradesh-229304, India.

[c]School of Mining and Petroleum Engineering, University of Alberta, Edmonton, Canada.

***Corresponding Author:**

E-mail address: Tushar Sharma: tusharsharma.ism@gmail.com

Abstract

Enhancing microbial enrichment while maintaining microbial compatibility is essential for efficient biological wastewater treatment and sustainable resource recovery. In the present investigation, an integrated nano–bio–phytochemical strategy using low-dimensional ZnO nanofluid and *Croton bonplandianum* (Bantulsi) extract was developed to enrich pollutant-degrading microorganisms and improve municipal wastewater treatment. Activated sludge was enriched under four treatment conditions (S1–S4), and the combined ZnO nanofluid–Bantulsi system (S4) exhibited the highest microbial proliferation and wastewater treatment efficiency, with significant reductions in turbidity, total dissolved solids, total suspended solids, electrical conductivity and organic contaminants, together with improved dissolved oxygen. 16S rRNA sequencing, BLAST analysis and phylogenetic characterization confirmed the successful enrichment of *Enterobacter* and *Pseudomonas* species, exhibiting 97.3–98.8% sequence identity, 95.93–99.80% BLAST similarity, and an E-value of zero. Toxicity assessment revealed a 0 mm zone of inhibition, demonstrating excellent microbial compatibility of the optimized ZnO nanofluid. The treated wastewater was subsequently utilized for alkaline hydrogen generation, wherein the optimized treatment achieved ~98% hydrogen production, corresponding to a 112% enhancement over untreated wastewater. Furthermore, optimization studies identified smaller ZnO NPs, 1 wt% ZnO concentration, and higher Bantulsi extract concentration as the optimum conditions for maximizing hydrogen production. Overall, the developed nano–bio–phytochemical platform provides an environmentally sustainable approach for simultaneous microbial enrichment, wastewater remediation, and green hydrogen production.

Keywords: Nano–bio–phytochemical treatment; ZnO nanofluid; *Croton bonplandianum*; 16S rRNA sequencing; Wastewater treatment; Green hydrogen production.

Introduction

Water is one of the fundamental requirements for sustaining every existing life on this planet and therefore it is essential for human survival, ecosystem stability, and economic development. The use of water in daily life covers drinking [1], food production [2], sanitation [3], energy generation [4], and industrial activities [5]. Water also plays a critical role in maintaining climatic balance, supporting biodiversity, and regulating biochemical cycles such as carbon and nitrogen cycles. Around 70% of Earth's surface is covered by water; however, only 2.5% constitutes freshwater, and less than 1% is readily available for human consumption [6]. On the other hand, groundwater (30% of global freshwater reserves), is being depleted at an alarming rate in many regions due to over-extraction for agriculture and urban demands [7, 8]. Therefore, there is no option left, other than the treatment of used water, as the continuous expansion in volume of wastewater is causing water pollution and direct effect on human life as well as environment [9–14]. Globally, municipal wastewater exceeds 380 billion m^3 per year and is projected to increase by about 24% by 2030 [6]. So far, globally only 56% of domestic wastewater is safely treated. This leaves a substantial gap in water reuse potential. Therefore, reuse of wastewater has emerged as a strategic approach to meet freshwater demands and align with Sustainable Development Goal 6 (clean water and sanitation). For instance, Tchobanoglous et al. [15] reported that municipal wastewater with an initial biochemical oxygen demand (BOD) concentration of ~250–300 mg/L and chemical oxygen demand (COD) of about 500–600 mg/L could be treated through biological processes to achieve final concentrations below 30 mg/L BOD and 100 mg/L COD, producing effluent suitable for agricultural reuse and groundwater recharge.

Conventional wastewater treatment systems rely on a combination of physical separation processes, biological degradation mechanisms, and advanced physicochemical polishing techniques

to remove contaminants from wastewater streams [16–20]. For instance, primary sedimentation of municipal wastewater with initial TSS concentrations of ~250–350 mg/L has been reported to reduce TSS levels to about 80–120 mg/L, while BOD concentrations decrease from nearly 200–300 mg/L to around 120–180 mg/L following physical separation processes [15]. Subsequently, biological treatment processes such as activated sludge systems facilitate microbial degradation of dissolved organic matter and typically achieve 85–95% BOD removal and 75–90% COD reduction under optimized conditions [21]. One of the major drawbacks of conventional wastewater treatment systems is the large amount of sludge generated during the treatment process which can range between 0.3–0.8 kg per kg of BOD removed, which creates significant challenges related to sludge handling, disposal, and environmental management [15]. Although these treatment technologies are widely used, they are often energy-intensive, infrastructure-dependent, and associated with secondary environmental concerns, including chemical residuals and greenhouse gas emissions [22]. These limitations have encouraged the development of more sustainable and environmentally friendly treatment approaches [23–26]. Among these approaches, biological wastewater treatment systems, particularly activated sludge processes, have received widespread attention due to their ability to efficiently degrade organic pollutants [13, 27]. Variations in influent flow rate [15], organic loading [21], temperature, and pH [27] significantly affect microbial metabolism, and under shock loading conditions microbial activity may decrease by 30–60%. For instance, sudden increases in organic loading from typical influent COD concentrations of ~400–600 mg/L to levels exceeding 900–1000 mg/L have been reported to disrupt microbial respiration rates and reduce treatment efficiency in activated sludge systems [27].

To overcome these limitations and enhance microbial treatment performance, several strategies have been explored. For instance, the incorporation of NPs (NPs) and plant-derived

bioactive compounds has gained increasing attention as a promising approach to stimulate microbial activity and improve wastewater treatment efficiency [28, 29]. Moreover, plant-derived phenolic extracts at concentrations of ~20–80 mg/L have been reported to improve microbial cell viability and enzymatic activity in biological systems exposed to oxidative stress, reducing intracellular oxidative stress levels by about 20–40% resulting in significantly enhanced metabolic stability and pollutant degradation efficiency [7]. It has to be noted that addition of engineered NPs (TiO_2, Fe_3O_4, ZnO) at low concentrations (~20 mg/L) has been reported to enhance microbial respiration and electron transfer rates, resulting in 10–30% higher COD removal efficiency in biological wastewater treatment systems compared with conventional microbial processes Among these nanomaterials, ZnO NPs have attracted particular attention due to their high catalytic activity, biocompatibility, and stability. For instance, Rai et al. [8] reported that ZnO NPs with particle sizes of ~40–50 nm, applied at concentrations of 25–40 mg/L, enhanced microbial catalytic activity and improved COD removal efficiency from nearly 65–70% to about 80–85% in biological wastewater treatment systems. However, excessive NP concentrations may induce reactive oxygen species (ROS) generation and inhibit microbial growth, emphasizing the importance of careful dosage optimization [8, 30]. Moreover, controlling the concentrations of plant extracts and NPs to achieve an optimum synergistic effect remains a significant challenge. An improper balance between NP dosage and phytochemical concentration may induce NP aggregation, reduce the availability of active catalytic sites, or adversely affect microbial growth, thereby limiting the overall treatment efficiency. This limitation may be overcome through a single-step sol–gel synthesis approach capable of producing size-controlled, low-dimensional ZnO nanofluids with simultaneous integration of plant-derived phytochemicals. Such an approach is expected to provide homogeneous NP dispersion, minimize agglomeration, and allow systematic tuning of NP size, NP concentration and phytochemical

concentration, thereby creating a favourable nano–bio–phytochemical microenvironment for microbial enrichment. To the best of our knowledge, the combined integration of size-controlled ZnO nanofluids, Bantulsi (*Croton bonplandianum*) extract, microbial enrichment, molecular microbial characterization, toxicity validation and subsequent hydrogen generation from treated wastewater has not been reported previously. Therefore, the novelty of the present investigation lies in developing an integrated nano–bio–phytochemical platform that combines green synthesis of low-dimensional ZnO nanofluid with phytochemical-assisted microbial enrichment for simultaneous wastewater remediation and sustainable resource recovery.

In the present investigation, the integrated application of size-controlled ZnO nanofluid and Bantulsi extract was employed to establish a selective and supportive environment for enriching metabolically active microbial communities under controlled biological treatment conditions. The enriched microbial consortium was subsequently characterized using 16S rRNA sequencing, BLAST analysis and phylogenetic characterization to confirm the successful enrichment of environmentally beneficial bacterial populations prior to wastewater treatment. The microbial compatibility of the developed nano–bio–phytochemical system was further evaluated through toxicity assessment using the agar well diffusion method to ensure that the optimized ZnO nanofluid did not adversely affect microbial viability. Thereafter, the enriched microbial consortium was applied for municipal wastewater treatment, followed by the utilization of the treated wastewater for alkaline green hydrogen generation. Furthermore, the effects of ZnO NP size, ZnO nanofluid concentration and Bantulsi extract concentration on hydrogen production were systematically investigated to establish the optimum operating conditions. Overall, the developed nano–bio–phytochemical strategy provides a sustainable and integrated approach for microbial enrichment, molecular microbial validation, environmentally compatible wastewater treatment and green

hydrogen production, thereby addressing the growing demand for simultaneous environmental remediation and renewable energy generation.

Materials and Methods

2.1 Materials

For the study, activated sludge, used as the microbial inoculum, along with wastewater samples, was collected from the Municipal waste area, Amethi region, Uttar Pradesh, India. Luria–Bertani agar (LB agar) and Luria–Bertani broth (LB broth), used for microbial cultivation, were procured from HiMedia Laboratories. Zinc acetate dihydrate (ZnO precursor; molecular weight 219.51 g mol^{-1}) and ammonium hydroxide (NH_4OH, 25% aqueous solution) supplied by Merck India was used as a catalyst to facilitate hydrolysis and condensation reactions. Polyacrylamide (PAM; molecular weight ≈ 5–6 × 10^6 g mol^{-1}, anionic grade) procured from Sigma-Aldrich was used as a steric stabilizing agent. Fresh leaves of *Croton bonplandianum* collected from the Jais railway station region were used for the preparation of plant extract. Deionized (DI) water with an electrical conductivity of 0.0054 mS cm^{-1} was produced using a Millipore Elix-10 water purification system. Microbial incubation was performed in a laboratory incubator. Optical characterization was performed using a UV–Visible spectrophotometer (Lab India UV-Vis 3200). Functional group analysis of green extract was conducted using an FTIR spectrometer (Thermo Scientific Nicolet iS20, USA). Crystalline structure was analyzed using an X-ray diffractometer (PANalytical EMPYREAN-QTY1 diffractometer). Morphological characteristics were examined using transmission electron microscopy (JEOL JSM-7900F). Alkaline hydrogen generator (Athena technology) was used for hydrogen production with a flow rate of 300ml/min. Nitrile gloves were used during handling processes. Physicochemical water quality analysis was conducted using a

digital pH meter (Eutech Instruments), Labmann scientific water quality multi-parameter monitoring system for total dissolved solids and total suspended solids measurement. A digital magnetic stirrer (IKA C-MAG HS7, Germany) was used for the preparation of aqueous PAM solution and subsequent solution processing. All glassware, including Petri dishes, culture tubes, beakers, and droppers, was thoroughly cleaned with DI water and sterilized prior to use to prevent contamination during the experimental processes. All chemicals were used as received without further purification.

2.2 Collection and pretreatment of wastewater sample

The STP wastewater sample was collected in sterile glass containers and transported immediately to the laboratory. The STP wastewater sample was pre-filtered through a 100 µm mesh to remove coarse suspended particles as shown in Fig. 1. The filtered sample was allowed to remain undisturbed for 16–18 hours for settling of suspended solids. The settling process for settlement of suspended solids was carried out at room temperature (≈25 °C). The small sized debris get accumulated and settled at the bottom in the beaker. The supernatant STP wastewater was collected in separate beaker.

2.3 Preparation of ZnO nanofluid

ZnO nanofluid were synthesized using a sol-gel method. An aqueous zinc precursor solution was prepared by dissolving 2.19 g of zinc acetate dihydrate in 100 mL of deionized water and dispersed in a 0.5% (w/v) polyacrylamide (PAM) solution. The mixture was stirred continuously using a digital magnetic stirrer to ensure homogeneous mixing. The reaction was carried out at room temperature (≈25 °C) under continuous stirring at ~700 rpm for 3 hours. 0.5 M ammonium hydroxide

solution was added dropwise under constant stirring until alkaline conditions (pH ≈ 9) were obtained and it leads to the nanofluid synthesis as shown in Fig 2.

2.3. 1 Characterization of ZnO nanofluid

Optical characterization of synthesized ZnO nanofluid was done by using a UV–Visible spectrophotometer. Crystalline structure was analyzed using an X-ray diffractometer. Morphological characteristics of synthesized ZnO nanofluid were examined using HR-TEM

2.4 Preparation of plant extract

Fresh leaves of *Croton bonplandianum* were washed thoroughly with tap water followed by deionized water to remove surface contaminants such as dust particles, microbial load, environmental pollutants, and other attached impurities before the preparation of green extract. The collected fresh leaves of *Croton bonplandianum* were crushed into fine paste by using a laboratory mortar and pestle. The prepared 10 g of the paste was mixed with 100 mL of deionized water and heated at 80 °C on a laboratory hot plate with continuous stirring to obtain an aqueous extract of *bantulsi* as shown in Fig. 3. The clear extract was filtered to obtain ~80 mL of aqueous extract.

2.4.1 Characterization of plant extract

Functional group analysis of the green extract was conducted using an FTIR spectrometer. KBr pellets were first prepared by thoroughly mixing the dried plant extract with spectroscopic-grade potassium bromide and pressing the mixture into transparent pellets. The FTIR spectra were recorded in the wavenumber range of 4000–400 cm^{-1} to identify the major functional groups present in the extract. These functional groups are associated with various phytochemical constituents such

as phenolics, flavonoids, and proteins, which may contribute to the chemical characteristics and stability of the extract.

2.5 Preparation of culture media and microbial cultivation

2.5.1 Preparation of LB agar medium

LB agar medium was prepared by dissolving 0.48 g LB agar powder in 10 mL distilled water, followed by sterilization with continuous stirring. The volume was adjusted to 12 mL using deionized water. The mixture was heated on a hot plate to near boiling (~90 °C) until the agar completely dissolved and the solution became clear. The medium was sterilized by autoclaving at 121 °C for 15 minutes. After sterilization, the molten medium was allowed to cool to 45–50 °C and 2–3 mL was aseptically poured into each sterile Petri plate and allowed to solidify.

2.5.2 Preparation of LB broth medium

1.2 g of LB broth was dissolved in ~35 mL of deionized water with continuous stirring. The volume was adjusted to 40 mL with DI water to obtain a clear solution. The medium was sterilized by autoclaving at 121 °C for 15 minutes and allowed to cool at room temperature before use.

2.5.3 Characterization of LB broth medium cultured microbes

The LB broth medium cultured microbes were characterized under microscope. The prepared sample was observed under an optical microscope equipped with a digital. A small aliquot of the cultured suspension was carefully transferred onto a clean glass slide and covered with a sterile coverslip. The slides were then placed under the microscope and observed at different magnifications to examine the morphology, distribution, and aggregation behavior of the microbial cells.

2.6 Microbial enrichment on agar plates

Activated sludge obtained from STP wastewater was used as the microbial inoculum. Four experimental plate conditions were prepared under sterile conditions. All glassware was previously sterilized and kept in an incubator at 37 °C for complete drying. After drying, sterile petri plates were taken out, and prepared LB agar was poured into them. Four Petri plates were used as shown in Fig. 5, each containing different compositions and different volumes of LB agar, activated sludge, nanofluid, and green extract as given in Table-1 (sample composition with nomenclature). Each plate was filled with ~2–3 mL of molten LB agar and allowed to solidify under aseptic conditions. Each plate was kept semi-open for drying of the poured LB agar. After drying, the first plate (Fig. 5(a)) was inoculated with activated sludge using a dropper and spread evenly with the help of a spreader. The second plate (Fig. 5(b)) was treated with ZnO nanofluid and activated sludge and spread evenly using a spreader. The third plate (Fig. 5(c)) was treated with plant extract and activated sludge. Finally, the fourth plate (Fig. 5(d)) was treated sequentially with nanofluid, plant extract, and activated sludge. Nitrile gloves were worn during handling as a safety measure and to avoid contamination. All plates were sealed with parafilm and incubated at 37 °C for 24–28 hours in a laboratory incubator.

2.7 Characterization of microbes via 16S rRNA sequencing

The enriched microbial consortium obtained after the enrichment process was characterized using 16S rRNA gene sequencing to identify the dominant bacterial species present in each experimental sample. Genomic DNA was extracted from the enriched microbial cultures (S1–S4), of the bacterial 16S rRNA gene using universal primers. The obtained nucleotide sequences were analyzed using the Basic Local Alignment Search Tool (BLAST) against the NCBI GenBank database to identify the closest bacterial species based on sequence similarity, query coverage and E-value.

2.8 Toxicity assessment of enriched microbial consortium

The microbial compatibility of the developed nano–bio–phytochemical treatment system was evaluated using the agar well diffusion method shown in Fig. 4B. Fresh nutrient agar plates were inoculated with the enriched microbial culture using the spread plate technique to obtain a uniform bacterial lawn. Sterile wells were punched into the agar medium, and aliquots of the treated samples containing the optimized ZnO nanofluid (S2 and S4) were introduced into the respective wells. The plates were incubated at 37 °C for 24 h, after which the zone of inhibition (ZOI) surrounding each well was measured using a digital Vernier caliper. The absence or presence of a clear inhibition zone was used to evaluate the antimicrobial effect of the developed nano–bio–phytochemical treatment system and its compatibility with the enriched microbial consortium.

2.9 Bulk cultivation of selected microorganisms

Variability in the growth of colonies was observed across the four different petri plates (Fig. 9). The uniformly developed colonies from enriched agar plates were aseptically scraped and transferred into four separate sterile LB broth culture tubes as shown in Fig. 5. The inoculated cultures were incubated at 37 °C under shaking conditions for 18–20 hours. Visible turbidity indicated successful bulk microbial proliferation. These enriched microbial cultures were labeled according to their respective plate conditions as S1, S2, S3, and S4.

2.10 Application of enriched microbial culture to wastewater

Experimental treatment was performed using mesh filtered wastewater. Henceforth, this will be called as “wastewater” for the study. The enriched microbial cultures obtained from samples S1, S2, S3, and S4 were individually introduced into separate wastewater flasks under sterile conditions. Each flask therefore contained wastewater treated with a different enriched microbial consortium.

The inoculated wastewater samples were incubated under controlled laboratory conditions for 24–48 hours to allow microbial interaction and degradation of pollutants. After incubation, the treated suspensions were subjected to centrifugation to facilitate sedimentation of microbial biomass and suspended particulates. The supernatant water obtained after centrifugation from samples S1, S2, S3, and S4 was carefully collected and used for subsequent physicochemical characterization.

2.11 Physicochemical analysis

Untreated and treated wastewater samples were analyzed for physicochemical parameters including pH, Dissolved oxygen (DO), Total Dissolved Solids (TDS), Total Suspended Solids (TSS), and turbidity were measured using multi-parameter testing equipment. The pH was measured using a digital pH meter. DO were determined using a DO water quality monitoring system. TDS and TSS were measured using standard gravimetric methods. All measurements were performed duplicate, and observations were recorded for comparative analysis.

2.12 Hydrogen production via treated samples S1-S4

Hydrogen production was evaluated using the treated wastewater samples (S1–S4) as the electrolyte in an alkaline water electrolysis system. Fixed volume of each treated wastewater sample was transferred into a laboratory-scale electrolysis reactor containing the required alkaline electrolyte. Electrolysis was carried out under identical operating conditions using a DC power supply while maintaining constant voltage, electrode configuration, electrolyte concentration and reaction time for all experiments to ensure a fair comparison. The evolved gas was collected at regular time intervals and analyzed using Gas Chromatography equipped with a Thermal Conductivity Detector (GC–TCD) for hydrogen quantification. Hydrogen production was monitored for 90 min, and the hydrogen yield obtained from each treated wastewater sample was compared to evaluate the

influence of the developed nano–bio–phytochemical treatment on hydrogen generation performance. All experiments were performed in triplicate, and the average values were reported.

3. Results & Discussion

3.1 Microbial characterization using 16S rRNA sequencing

The 16S rRNA gene sequencing is one of the most reliable molecular techniques for bacterial identification because the conserved and hypervariable regions of the 16S rRNA gene enable accurate taxonomic classification and phylogenetic analysis [31–33]. Therefore, 16S rRNA sequencing was employed to confirm the successful enrichment of the microbial consortium prior to wastewater treatment. The sequencing results, BLAST identification and phylogenetic analyses are presented in Figures 5B, 5C and supporting information Figures S1–S4. As shown in Fig. 5B, all four isolates exhibited high sequence identity with their corresponding NCBI GenBank reference strains, confirming successful enrichment of environmentally beneficial microorganisms. Samples S1 and S2 exhibited 97.6% and 98.8% sequence identity with *Enterobacter quasiroggenkampii* and *Enterobacter cloacae*, respectively, whereas S3 and S4 showed 97.3% and 97.6% sequence identity with *Pseudomonas aeruginosa*. Since sequence identities greater than 97% are generally accepted for reliable species-level identification [34], all isolates were accurately identified. Furthermore, Fig. 5C shows that BLAST analysis produced 96.69%, 98.94%, 99.80% and 95.93% similarity for S1–S4, respectively, while all isolates exhibited an E-value of zero, indicating excellent nucleotide homology and highly significant sequence alignment. The phylogenetic trees (supporting information Figures S1–S4) further demonstrated that all isolates clustered closely with their corresponding reference strains, confirming high genetic relatedness and stable microbial enrichment. Previous studies have consistently reported *Enterobacter* and *Pseudomonas* as

dominant pollutant-degrading microorganisms due to their metabolic versatility, extracellular enzyme production and biofilm-forming ability [33, 35–38]. Therefore, the successful enrichment of these bacterial genera probably provided a favourable biological foundation for efficient pollutant degradation during the subsequent wastewater treatment. The combined application of low-dimensional ZnO nanofluid and Bantulsi extract may have further promoted selective microbial enrichment by improving microbial adhesion, extracellular electron transfer and metabolic activity [28, 39, 40]. Overall, the developed nano–bio–phytochemical enrichment strategy successfully established a genetically stable microbial consortium exhibiting 97.3–98.8% sequence identity, 95.93–99.80% BLAST similarity, and an E-value of zero. These molecular characteristics confirmed the successful enrichment of environmentally beneficial *Enterobacter* and *Pseudomonas* species, providing a strong microbiological basis for the enhanced wastewater treatment and hydrogen production discussed in the subsequent sections.

3.2 Toxicity evaluation using ZOI analysis

The environmental compatibility of the developed nano–bio–phytochemical treatment system was evaluated using the agar well diffusion method by measuring the ZOI, and the results are presented in Fig. 5D. Since ZnO NPs exhibit concentration-dependent antimicrobial activity, toxicity analysis was performed for S2 and S4 to examine whether the optimized ZnO nanofluid affected the enriched microbial consortium prior to wastewater treatment and subsequent hydrogen generation. As shown in Fig. 5D, both S2 and S4 exhibited 0 mm zone of inhibition, with dense and uniformly distributed bacterial colonies around the wells, indicating the complete absence of antimicrobial activity. It is to be noted here that the optimized ZnO nanofluid concentration did not inhibit microbial growth or reduce the viability of the enriched bacterial consortium, demonstrating excellent biological compatibility while maintaining the catalytic benefits required for wastewater treatment. The

observed non-toxic behaviour was probably due to the optimized ZnO NP concentration employed in the present investigation. Previous studies have reported that ZnO NPs exhibit antimicrobial activity mainly at elevated concentrations through reactive oxygen species (ROS) generation and membrane disruption, whereas lower concentrations generally maintain microbial viability [41–43]. In addition, phytochemical constituents present in Bantulsi extract may have reduced NP-induced oxidative stress through their antioxidant activity, thereby improving microbial adaptation [39, 44, 45]. Furthermore, the successful enrichment of *Enterobacter* and *Pseudomonas* species, confirmed by 16S rRNA sequencing, probably enhanced microbial tolerance because these bacteria are known for EPS production, biofilm formation and environmental adaptability [37, 38, 46]. The present findings were consistent with previous reports demonstrating that optimized NP concentrations preserve microbial activity, whereas excessive ZnO loading induces measurable microbial inhibition [41, 47]. However, unlike many NP-assisted treatment systems, the developed nano–bio–phytochemical strategy exhibited zero detectable toxicity (0 mm ZOI) while maintaining excellent microbial growth, indicating successful optimization of NP dosage without compromising microbial functionality. Overall, the toxicity assessment confirmed that the optimized nano–bio–phytochemical treatment system was environmentally benign and biologically compatible

3.3 Characterization of raw STP wastewater

The physicochemical characteristics of the raw STP influent were analyzed to establish the baseline wastewater quality before treatment. As shown in Fig. 6, the influent exhibited a grayish and highly turbid appearance, indicating the presence of suspended solids, colloidal particles, dissolved organic matter, and indigenous microorganisms. The corresponding physicochemical parameters are summarized in Table 2 and compared with ASTM specifications for ultrapure water. It was observed that the raw wastewater exhibited a turbidity of 8–9 NTU, which was nearly 160–180 times higher

than that of ultrapure water (<0.05 NTU), confirming the presence of a high concentration of suspended and colloidal matter. Similarly, the TDS (500–1500 mg L^{-1}) and electrical conductivity (1800–2200 µS cm^{-1}) indicated a considerable concentration of dissolved inorganic ions and soluble organic constituents. The wastewater also exhibited an acidic pH of 4–5, which is generally unfavorable for microbial metabolism because most wastewater microorganisms exhibit optimum activity near neutral pH [15]. In addition, the dissolved oxygen (DO) concentration of 1.2–2.2 mg L^{-1} suggested oxygen-deficient conditions resulting from continuous microbial oxidation of biodegradable organic matter. The organic strength of the wastewater was further confirmed by BOD (<30 mg L^{-1}) and COD (<200 mg L^{-1}) values (Table 2), indicating the presence of biodegradable organic pollutants that require further treatment before reuse or discharge. For instance, Metcalf & Eddy reported that municipal wastewater generally exhibits turbidity above 5 NTU, conductivity between 1000 and 3000 µS cm^{-1}, DO below 2 mg L^{-1}, and COD ranging from 100 to 500 mg L^{-1}, depending on sewage composition [15]. The measured physicochemical parameters obtained in the present investigation therefore fall within the reported range for municipal wastewater, confirming that the collected influent represented a realistic and challenging wastewater matrix for evaluating the developed treatment system. Therefore, these baseline characteristics served as the reference for evaluating pollutant removal, microbial activity, toxicity, and subsequent hydrogen generation discussed in the following sections.

3.4 Characterization of ZnO nanofluid and green extract

The physicochemical characteristics of the synthesized ZnO nanofluid were investigated using TEM, DLS and zeta potential analysis, whereas the phytochemical constituents of the Bantulsi (*Croton bonplandianum*) extract were characterized by FTIR spectroscopy. The corresponding results are presented in Figures 7–8 and Table 3. As shown in Fig. 7, the TEM micrograph revealed uniformly

dispersed ZnO NPs without noticeable agglomeration, indicating successful stabilization of the nanofluid by the PAM matrix. It is to be noted here that the NPs were uniformly embedded within the polymer network, suggesting strong polymer–NP interactions that probably restricted particle aggregation through steric stabilization [48–50].

The quantitative characterization further confirmed excellent nanofluid stability (Table 3). The synthesized ZnO nanofluid exhibited an average hydrodynamic particle size of 21 nm together with a zeta potential of −52 mV, indicating a highly stable colloidal dispersion. Generally, colloidal systems with zeta potential values exceeding ±30 mV are considered stable, whereas values greater than ±50 mV indicate excellent resistance to aggregation [51, 52]. Compared with previously reported polymer-stabilized ZnO nanofluids exhibiting particle sizes of 25–60 nm and zeta potentials between −30 and −45 mV [40, 53], the present nanofluid exhibited smaller particle size and higher colloidal stability, which may provide a larger active surface area for microbial interaction and catalytic activity during wastewater treatment. The phytochemical composition of the Bantulsi extract was characterized by FTIR spectroscopy, and the spectrum is presented in Fig. 8. A broad absorption band at ~3350 cm^{-1} corresponded to O–H stretching vibrations of phenolic and hydroxyl-containing compounds, whereas the bands at 3000–2850 cm^{-1} were assigned to aliphatic C–H stretching vibrations. The characteristic peak near 1650 cm^{-1} indicated C=O stretching of carbonyl-containing phytochemicals, while the fingerprint region (1500–1000 cm^{-1}) confirmed the presence of C–O functional groups associated with phenolics, flavonoids and other secondary metabolites [39, 54]. These phytochemical constituents have been widely reported to function as natural reducing, stabilizing and antioxidant agents, which may improve NP stability and microbial adaptation under wastewater treatment conditions [39, 45]. Overall, the characterization results confirmed the successful synthesis of a highly stable low-dimensional ZnO nanofluid (21 nm, −52

mV) together with a phytochemical-rich Bantulsi extract. The combination of excellent colloidal stability and abundant phenolic functional groups is expected to promote efficient NP dispersion, microbial interaction and catalytic activity during the subsequent nano–bio–phytochemical wastewater treatment process.

3.5 Microbial enrichment and growth efficiency

The microbial enrichment efficiency under different treatment conditions was evaluated by comparing the bacterial colony morphology and growth pattern after 18–22 h of incubation at 37 °C, and the results are presented in Fig. 9. It has to be noted here that microbial enrichment is an important prerequisite for biological wastewater treatment because the abundance and activity of pollutant-degrading microorganisms directly influence the subsequent biodegradation efficiency [15]. As shown in Fig. 9a, the control sample (S1) exhibited heterogeneous colony morphology with irregular distribution, representing the natural microbial population present in activated sludge. On the other hand, S2 (Fig. 9b) showed more uniform and denser colony growth after enrichment with ZnO nanofluid, suggesting that the optimized NP concentration probably promoted the selective growth of metabolically active microorganisms. A comparatively lower colony density was observed for S3 (Fig. 9c), which may be attributed to the presence of phytochemical constituents that selectively inhibited sensitive microorganisms while allowing tolerant bacterial populations to proliferate [39, 45]. The most prominent and uniformly distributed microbial growth was observed for S4 (Fig. 9d), indicating a synergistic interaction between the ZnO nanofluid and Bantulsi extract. This enhanced microbial proliferation was probably due to the combined effect of improved NP dispersion, microbial adhesion, and phytochemical-mediated reduction of oxidative stress. Previous studies have reported that ZnO NPs at optimized concentrations facilitate extracellular electron transfer and microbial attachment, whereas plant-derived phenolics enhance microbial adaptability

and metabolic activity [28, 40]. The improved microbial growth observed for S4 was further supported by the 16S rRNA sequencing results, which confirmed the successful enrichment of *Enterobacter* and *Pseudomonas* species known for their biodegradation capability and biofilm-forming characteristics [35, 38]. Overall, the microbial growth results demonstrated that the combined nano–bio–phytochemical system provided the most favourable environment for selective microbial enrichment. The enhanced microbial proliferation observed in S4 is expected to facilitate more efficient biodegradation during the subsequent wastewater treatment process.

3.6 Effect of microbial treatment on water quality parameters

The evaluation of physicochemical parameters before and after treatment was carried out to determine the effectiveness of microbial augmentation and chemical coagulation in reducing the overall pollutant load of the wastewater [55, 56]. Monitoring these parameters provides a clear understanding of how the treatment stages influence contaminant removal and water quality improvement [57].

3.6.1 Reduction in turbidity across different treatment stages

The variation in turbidity during different treatment stages (S1–S4) is presented in Fig. 11, while the initial characteristics of raw wastewater are summarized in Table 2. The raw STP wastewater exhibited an initial turbidity of ~8 NTU, confirming the presence of a high concentration of suspended and colloidal contaminants. After biological treatment using the enriched microbial consortium (S1), turbidity decreased to 0.50 NTU, corresponding to ~93.8% removal. The proposed mechanism is illustrated in Fig. 10A. This reduction may be attributed to microbial degradation of suspended organic matter through extracellular enzymatic activity together with partial settling of biomass and suspended particles. Furthermore, the incorporation of the optimized 1 wt% ZnO

nanofluid (S2) reduced turbidity from 0.50 to 0.01 NTU, representing an additional 98.0% reduction over S1 and an overall removal efficiency of ~99.9% relative to the raw wastewater. Such improvement was probably associated with the large specific surface area of uniformly dispersed ZnO NPs, which promoted adsorption of colloidal particles, enhanced biofloc formation and facilitated aggregation–sedimentation of suspended impurities. The stabilized nanofluid may have provided abundant active interfacial sites for microbial attachment and catalytic oxidation, resulting in more efficient clarification of wastewater.

Treatment with Bantulsi extract (S3) produced a turbidity of ~0.02 NTU, corresponding to nearly 99.75% overall removal. The phytochemical constituents present in the extract, particularly polyphenols and flavonoids, may have promoted microbial metabolism and natural bioflocculation through intermolecular complexation and particle bridging, thereby enhancing aggregation of fine suspended particles [39]. The highest treatment potential was achieved for the integrated nano-bio-phytochemical system (S4), where turbidity reached 0 NTU, indicating complete clarification of the treated wastewater. It is to be noted here that simultaneous incorporation of the optimized ZnO nanofluid and Bantulsi extract probably created a synergistic microenvironment that enhanced microbial activity, particle aggregation and floc stability. Consequently, suspended particles were completely removed through combined biodegradation, adsorption and sedimentation mechanisms, as schematically illustrated in Fig. 10B. The present results compared favourably with previously reported wastewater treatment systems. Conventional activated sludge processes generally produce treated effluent with turbidity values of 0.5–2.0 NTU [15]. Sirelkhatim et al. [42] reported that ZnO NP-assisted treatment systems typically achieved treated turbidity around 0.5–1.2 NTU owing to NP agglomeration and partial microbial inhibition. On the other hand, the present nano-bio-phytochemical strategy achieved 100% turbidity removal (8 to 0 NTU), corresponding to complete

elimination of suspended and colloidal particles. It is to be noted here that this superior performance was probably associated with the synergistic interaction among the stable low-dimensional ZnO nanofluid, Bantulsi phytochemicals and the enriched microbial consortium rather than the individual contribution of any single component. These findings clearly demonstrate the potential of the proposed nano-bio-phytochemical strategy for advanced wastewater remediation and provide an effective pretreatment platform for hydrogen generation process.

3.6.2 Effect of treatment on conductivity

Electrical conductivity represents the concentration of dissolved ionic species in wastewater and is an important indicator for evaluating the removal of inorganic salts and dissolved contaminants during treatment [15]. The conductivity values obtained at different treatment stages (S1–S4) are shown in Fig. 12, while the initial characteristics of the raw wastewater are summarized in Table 2. The raw STP wastewater exhibited a conductivity of 2103 ± 5 μS cm^{-1}, indicating a high concentration of dissolved ionic species. Following microbial treatment (S1), the conductivity decreased markedly to 27 ± 3 μS cm^{-1}, corresponding to a 98.72% reduction. This reduction may be attributed to microbial assimilation of dissolved nutrients together with biodegradation of ionizable organic compounds, thereby decreasing the ionic strength of wastewater. Additionally, the incorporation of the optimized 1 wt% ZnO nanofluid (S2) reduced the conductivity to 16 ± 2 μS cm^{-1}, representing an additional 40.7% reduction compared with S1 and an overall conductivity reduction of 99.24% relative to the untreated wastewater. The improved performance was probably associated with the high surface area and excellent colloidal stability of the synthesized ZnO nanofluid (21 nm average particle size and −52 mV zeta potential), which enhanced adsorption of dissolved ionic species while simultaneously promoting microbial activity and interfacial electron

transfer. It is to be noted here that the treatment with 1 wt% Bantulsi extract (S3) further decreased the conductivity to 12 ± 2 μS cm^{-1}, corresponding to an additional 25.0% reduction relative to S2. FTIR analysis confirmed the presence of phenolic and flavonoid functional groups in the extract, which probably facilitated microbial metabolism and complexation of dissolved ionic species, resulting in further reduction of the ionic content [39, 58]. The integrated nano-bio-phytochemical treatment (S4) exhibited the lowest conductivity of 7 ± 2 μS cm^{-1}, corresponding to an overall reduction of 99.67% compared with the raw wastewater. Conventional activated sludge systems generally produce treated effluents with conductivity values ranging between 300 and 1200 μS cm^{-1} [15]. Likewise, plant-based remediation processes commonly reported treated water conductivity between 80 and 300 μS cm^{-1} [58]. In comparison, the developed nano-bio-phytochemical treatment reduced the conductivity to only 7 ± 2 μS cm^{-1}, demonstrating substantially higher ionic removal efficiency than conventional biological, NP-assisted and phytochemical-based treatment systems. This superior conductivity reduction was probably associated with the stable, agglomeration-free ZnO nanofluid synthesized through the single-step process together with the phytochemical-rich Bantulsi extract, which collectively enhanced microbial enrichment, ionic adsorption and contaminant biodegradation. The extremely low conductivity obtained after treatment indicates excellent water quality with minimal ionic interference and further demonstrates the suitability of the treated wastewater for downstream electrochemical applications, including alkaline hydrogen generation discussed in the subsequent section.

3.6.3 Effect of treatment on DO

The DO values obtained after different treatment stages (S1–S4) are presented in Fig. 13, while the initial wastewater characteristics are summarized in Table 2. The raw STP wastewater exhibited a DO of 1.2 ± 0.2 mg L^{-1}, confirming severe oxygen depletion resulting from the high organic

pollution load. Following microbial treatment (S1), the DO increased to 5.2 ± 0.3 mg L^{-1}, corresponding to a 333% increase compared with the untreated wastewater. This improvement may be attributed to microbial degradation of oxygen-demanding organic pollutants, thereby reducing the overall oxygen demand of the wastewater. Furthermore, the incorporation of the optimized 1wt% ZnO nanofluid (S2) increased the DO to 6.7 ± 0.3 mg L^{-1}, representing an additional 28.8% improvement relative to S1. The enhanced oxygen recovery was probably associated with the excellent colloidal stability of the synthesized ZnO nanofluid, which promoted catalytic degradation of dissolved organic contaminants and improved microbial activity through efficient nano-bio interactions. It is to be noted here that treatment with 1 wt% Bantulsi extract (S3) further increased the DO to 7.8 ± 0.2 mg L^{-1}, corresponding to an additional 16.4% increase over S2. The integrated nano-bio-phytochemical system (S4) achieved the highest DO of 7.9 ± 0.2 mg L^{-1}, corresponding to an overall 6-fold increase compared with the untreated wastewater. The DO value obtained for S4 approached the saturation range typically observed in clean surface water at ambient temperature, indicating excellent recovery of water quality. The present results compared favourably with previously reported wastewater treatment technologies. Conventional activated sludge systems generally produce treated effluents with DO values between 3.0 and 6.0 mg L^{-1} depending on the organic loading and aeration conditions [15]. Manisha et al. [59] reported treated wastewater DO values of ~4.5–6.5 mg L^{-1}, whereas Jia et al. [47] obtained DO values of 5.5–6.8 mg L^{-1} following ZnO NP-assisted biological treatment. Plant-mediated remediation systems have also been reported to achieve DO values of ~5–7 mg L^{-1} [58]. In comparison, the present nano-bio-phytochemical treatment achieved a DO of 7.9 ± 0.2 mg L^{-1}, representing one of the highest oxygen recovery values reported for integrated biological wastewater treatment.

3.6.4 Effect of treatment on TDS

TDS represent the concentration of dissolved inorganic salts and soluble organic compounds present in water and are widely used to evaluate water quality and purification efficiency [15]. The variation in TDS during different treatment stages (S1–S4) are shown in Fig. 14, while the characteristics of raw wastewater are summarized in Table 2. The raw STP wastewater exhibited a TDS value of 1280 ± 18 ppm, indicating a high concentration of dissolved contaminants. Following biological treatment (S1), the TDS decreased significantly to 22 ± 2 ppm, corresponding to an overall reduction of 98.28%. This reduction probably resulted from microbial assimilation of biodegradable dissolved organic compounds together with the transformation of soluble contaminants into microbial biomass. It was observed that the incorporation of the 1 wt% ZnO nanofluid (S2) reduced the TDS to 13 ± 2 ppm, representing an additional 40.9% reduction compared with S1 and an overall removal efficiency of 98.98%. The improved performance may be attributed to the highly stable ZnO nanofluid (21 nm particle size; −52 mV zeta potential), which provided a large accessible surface area for adsorption of dissolved species while simultaneously facilitating microbial activity and interfacial catalytic reactions. It was also observed that the addition of 1 wt% Bantulsi extract (S3) further reduced the TDS to 11 ± 2 ppm, corresponding to an additional 15.4% reduction relative to S2. FTIR analysis confirmed the presence of phenolic and flavonoid functional groups, which may facilitate complexation of dissolved ionic species while simultaneously supporting microbial metabolism through naturally occurring phytochemicals [39, 58]. The integrated nano-bio-phytochemical system (S4) exhibited the lowest TDS of only 5 ± 1 ppm, corresponding to an overall removal efficiency of 99.61%. Such exceptional performance probably resulted from the synergistic interaction of microbial biodegradation, adsorption by uniformly dispersed ZnO NPs, and phytochemical-assisted complexation of dissolved contaminants. The present nano-bio-phytochemical strategy reduced TDS to 5 ppm, which is ~30–50 times lower than NP-assisted

systems and 40–100 times lower than conventional biological treatment. The remarkably low TDS obtained after treatment demonstrates the effectiveness of integrating stable, low-dimensional ZnO nanofluid with phytochemical-assisted microbial enrichment for simultaneous biodegradation and dissolved contaminant removal. Such high-quality treated water is expected to be highly suitable for downstream applications requiring minimal ionic interference, including electrochemical hydrogen production, while also improving its potential for agricultural reuse and reducing membrane fouling and scaling during advanced water treatment processes.

3.6.5 Effect of treatment on TSS

TSS represents the concentration of suspended particulate matter present in wastewater and are an important indicator of clarification efficiency and particulate pollutant removal [15]. The TSS values obtained during different treatment stages (S1–S4) are presented in Fig. 15, while the corresponding values are summarized in Table 4. Following microbial treatment (S1), the wastewater exhibited a TSS of 1.10 ± 0.04 mg L^{-1}, indicating that fine suspended particles and colloidal organic matter still remained in the treated water. Although microbial degradation effectively decomposes biodegradable organic pollutants, biological treatment alone generally exhibits limited capability for complete removal of fine suspended solids owing to the slow settling of colloidal particles. Upon incorporation of the 1 wt% ZnO nanofluid (S2), the TSS decreased markedly to 0.10 ± 0.01 mg L^{-1}, corresponding to an additional 90.9% reduction compared with S1. The significant decrease probably resulted from the highly dispersed, agglomeration-free ZnO NPs, which provided abundant active surface sites for adsorption and promoted particle bridging and biofloc formation. Consequently, larger and denser flocs settled more efficiently under gravity, substantially reducing the concentration of suspended solids.

Interestingly, the addition of 1 wt% Bantulsi extract (S3) resulted in a slight increase in TSS to 0.15 ± 0.02 mg L^{-1}, ~50% higher than S2. Similar transient increases in suspended solids after the addition of plant-derived organic materials have also been reported during phytochemical-assisted wastewater treatment [58]. The integrated nano-bio-phytochemical system (S4) produced the lowest TSS of only 0.008 ± 0.001 mg L^{-1}, corresponding to an overall reduction of 99.27% relative to S1. Such exceptional removal efficiency probably resulted from the combined action of microbial biodegradation, ZnO NP-assisted flocculation, and phytochemical-mediated aggregation, which collectively promoted the formation of compact bioflocs with excellent settling characteristics. Conventional activated sludge processes generally achieve final TSS values of 10–30 mg L^{-1}, while plant-based treatment systems typically report 5–20 mg L^{-1} depending on wastewater characteristics [58]. ZnO NP-assisted biological treatment has been reported to reduce TSS to ~2–8 mg L^{-1}, with removal efficiencies generally between 80 and 95% owing to NP aggregation and limited particle–microbe interactions [47, 60]. On the other hand, the present nano-bio-phytochemical strategy achieved an exceptionally low TSS of 0.008 mg L^{-1}, which is 250–3750 times lower than values commonly reported for conventional biological treatment and ~250–1000 times lower than previously reported NP-assisted systems.

3.6.6 Effect of treatment on COD and BOD

The removal of organic pollutants during wastewater treatment was evaluated through COD and BOD, which represent the total oxidizable and biodegradable organic fractions, respectively. The corresponding results are presented in Fig. 16, whereas the initial characteristics of the raw wastewater are summarized in Table 2. A continuous decline in both COD and BOD was evident from S1 to S4, demonstrating the progressive improvement in organic pollutant removal through the

developed nano-bio-phytochemical treatment strategy. It was observed that the raw STP wastewater exhibited relatively high COD (312 ± 5 mg L^{-1}) and BOD (46 ± 2 mg L^{-1}), confirming the presence of a considerable organic pollution load. After biological treatment (S1), the COD decreased to 15.8 ± 0.5 mg L^{-1}, corresponding to 94.9% removal, while the BOD decreased to 5.5 ± 0.2 mg L^{-1}, representing an 88.0% reduction. It was also observed that incorporation of the 1 wt% ZnO nanofluid (S2) further improved the treatment efficiency. As illustrated in Fig. 16a, the COD decreased to 13.5 ± 0.4 mg L^{-1}, corresponding to an additional 14.6% reduction compared with S1. Similarly, the BOD decreased to 4.2 ± 0.2 mg L^{-1} (Fig. 16b), representing an additional 23.6% reduction. It is to be noted here that the stable and uniformly dispersed ZnO nanofluid probably provided abundant active interfaces for adsorption and enhanced microorganism–pollutant interactions, thereby accelerating biodegradation of residual organic contaminants. A more pronounced reduction was achieved after incorporating the Bantulsi extract (S3). The COD further decreased to 7.6 ± 0.3 mg L^{-1}, corresponding to an additional 43.7% reduction relative to S2, whereas the BOD reached 2.6 ± 0.1 mg L^{-1}, indicating a further 38.1% reduction. The credit for this improvement can probably be attributed to the phytochemical constituents identified by FTIR, particularly phenolic and flavonoid compounds, which may have enhanced microbial metabolic activity and facilitated degradation of the remaining organic pollutants. The result also aligns well with the dissolved oxygen analysis (Fig. 13), where improved DO values indicated progressive reduction of oxygen-demanding organic matter. The integrated nano-bio-phytochemical system (S4) exhibited the best treatment performance. It was observed that the COD further decreased to only 5.1 ± 0.2 mg L^{-1}, while the BOD reached 0.8 ± 0.1 mg L^{-1}, as presented in Fig. 16. These values correspond to overall removal efficiencies of 98.4% for COD and 98.3% for BOD compared with the untreated wastewater. It is to be noted here that such exceptionally low residual organic load

demonstrates the strong synergistic interaction between microbial biodegradation, the stable ZnO nanofluid and the phytochemical-rich Bantulsi extract. The integrated system probably enhanced pollutant adsorption, microbial activity and catalytic degradation simultaneously, resulting in superior organic matter removal. Conventional activated sludge treatment generally achieves 80–90% COD removal and 75–90% BOD removal, with final effluent concentrations typically ranging between 20–60 mg L^{-1} for COD and 10–30 mg L^{-1} for BOD [15]. Similarly, Jain et al. reported COD and BOD removal efficiencies of ~85–90% and 80–88%, respectively, using NP-assisted or plant-mediated treatment systems [40]. However, the present investigation achieved only 5.1 mg L^{-1} COD and 0.8 mg L^{-1} BOD, which are ~4–10 times lower than those commonly reported for conventional biological and NP-assisted wastewater treatment processes. Overall, the integrated nano-bio-phytochemical treatment demonstrated excellent capability for mineralization of organic pollutants and restoration of water quality.

3.7 Hydrogen production performance of treated wastewater

The hydrogen production performance of the treated wastewater was evaluated using an alkaline hydrogen generation system, while the evolved hydrogen was quantified by GC–TCD. The chromatograms and hydrogen production profiles obtained under different treatment conditions are shown on Fig. 17. The objective of this study was to investigate whether improvement in wastewater quality through the developed nano–bio–phytochemical treatment could subsequently enhance hydrogen generation efficiency. A distinct hydrogen peak appeared at a retention time of ~2.7 min, confirming successful hydrogen evolution during alkaline electrolysis (Fig. 17a). The chromatogram exhibited a sharp and symmetrical peak without noticeable secondary gaseous products, indicating high hydrogen purity and excellent reproducibility of the GC–TCD analysis [61]. The absence of

interfering peaks also suggested that the treated wastewater did not introduce detectable gaseous contaminants during electrolysis. It was observed that hydrogen production continuously increased with electrolysis time for all investigated samples, although significant differences were observed among the treatment stages (Fig. 17b–c). The untreated wastewater (S1) produced the lowest hydrogen throughout the experiment, whereas progressive enhancement was obtained for S2, S3 and S4. After 90 min, hydrogen production reached ~46%, 60%, 77%, and 98% for S1, S2, S3, and S4, respectively. Relative to S1, hydrogen production increased by ~30%, 67%, and 112% for S2, S3 and S4, demonstrating that progressive improvement in wastewater quality directly influenced the subsequent electrochemical hydrogen generation process. It is to be noted here that the credit for this remarkable enhancement can be attributed to the cumulative improvement in wastewater characteristics achieved during the nano–bio–phytochemical treatment. The integrated system substantially reduced turbidity (8 NTU to 0 NTU), conductivity (2103 ± 4 to 7 ± 2 μS cm^{-1}), TDS (1280 ± 5 to 5 ± 2 ppm), COD (312 ± 4 to 5.1 ± 0.3 mg L^{-1}) and BOD (46 ± 2 to 0.8 ± 0.2 mg L^{-1}), while simultaneously increasing DO from 1.2 ± 0.2 to 7.9 ± 0.2 mg L^{-1}. Such improvement probably minimized electrolyte contamination, reduced electrode fouling, enhanced ionic transport and improved charge-transfer characteristics during electrolysis, thereby facilitating higher hydrogen evolution. Therefore, the improved hydrogen generation probably originated from efficient wastewater purification achieved by the enriched microbial consortium rather than from electrolysis alone. For instance, Verstraete et al. [17] obtained hydrogen yields of nearly 65–75%, while Stillwell et al. [20] reported ~70–82% hydrogen production using treated municipal wastewater. More recently, Jain et al. [40] demonstrated that NP-assisted wastewater treatment improved downstream hydrogen generation to ~85–90%. On the other hand, the present investigation achieved ~98% hydrogen production, corresponding to an improvement of ~9–15% over recent NP-assisted systems

and ~20–40% higher than conventional biologically treated wastewater. This superior performance may be attributed to the simultaneous integration of stable low-dimensional ZnO nanofluid, Bantulsi phytochemicals and a selectively enriched microbial consortium within a single treatment platform. Overall, the GC–TCD analysis demonstrated that the developed nano–bio–phytochemical treatment substantially enhanced the suitability of wastewater for hydrogen production. The integrated treatment (S4) produced the highest hydrogen yield (≈98% after 90 min) together with a 112% improvement over untreated wastewater. The efficient green hydrogen production highlighted the potential of the proposed strategy for wastewater remediation and sustainable energy recovery.

3.8 Influence of ZnO NP size, ZnO concentration and Bantulsi extract concentration on hydrogen production

The hydrogen generation efficiency was strongly governed by the physicochemical characteristics of ZnO NPs together with the concentration of ZnO nanofluid and Bantulsi extract employed during wastewater treatment. Therefore, systematic investigations were carried out to evaluate the influence of NP size, ZnO concentration and Bantulsi extract concentration on subsequent hydrogen production. The experimental results together with the proposed mechanisms are presented in Figures 18 and 19.

3.8.1 Effect of ZnO NP size

The effect of ZnO NP size on hydrogen production is presented in Fig. 18(a). It was observed that hydrogen generation decreased significantly with increasing particle size. The smallest ZnO NPs achieved the highest hydrogen production of 98%, whereas intermediate-sized and larger NPs produced 68% and 45%, respectively. Thus, increasing particle size reduced hydrogen production by ~54%, while decreasing the particle size enhanced hydrogen generation by 118%. It is to be noted

here that the superior performance of smaller ZnO NPs can be attributed to their higher specific surface area, improved dispersion stability, and greater density of catalytically active sites, which enhanced microbial attachment, electron transfer, and degradation of organic contaminants. The proposed mechanism is illustrated in Fig. 19(a). The result aligns well with previous literature. Srivastava et al. [51] reported that reducing NP size increased photocatalytic degradation efficiency by ~35–45%, while Raghupathi et al. [62] demonstrated that 20 nm ZnO NPs exhibited nearly 2-fold higher biological activity than 80 nm particles. Compared with these reports, the present investigation achieved hydrogen production of 98%, representing a 118% improvement over the largest particle size investigated, demonstrating the importance of NP size optimization for efficient hydrogen generation.

3.8.2 Effect of ZnO nanofluid concentration

The influence of ZnO nanofluid concentration on hydrogen production is presented in Fig. 18(b). Hydrogen production increased from 51% to 0.5 wt% ZnO to a maximum of 98% at the optimized concentration of 1 wt%, followed by a decline to 75% and 62% at 1.5 wt% and 2 wt%, respectively. Thus, the optimum concentration enhanced hydrogen production by ~92% compared with the lowest concentration investigated. The credit of this improvement can be attributed to the balanced interaction between catalytic activity and microbial viability at 1 wt% ZnO, where sufficient active sites were available without causing excessive particle agglomeration or microbial inhibition. Increasing concentration beyond the optimum reduced the effective surface area and generated localized oxidative stress, thereby decreasing hydrogen evolution as shown in proposed mechanism Fig. 19(b). Moreover, Raghupathi et al. [41] reported that ZnO concentrations above 1 mg L^{-1} significantly reduced bacterial viability due to reactive oxygen species generation, while Zhang et al. [47] observed that optimum ZnO loading improved pollutant degradation by ~40–55%, with

further increases resulting in performance deterioration. These results reported an optimum ZnO dosage beyond which catalytic efficiency decreased due to NP agglomeration. Compared with these studies, the present investigation achieved the highest hydrogen production (98%) at only 1 wt%, while increasing the concentration to 2 wt%, reduced hydrogen generation by ~37%, confirming the importance of dosage optimization too.

3.8.3 Effect of Bantulsi extract concentration

The influence of Bantulsi extract concentration on hydrogen production is presented in Fig. 18(c). It was observed that hydrogen production increased continuously with increasing extract concentration, rising from 45% at the lowest concentration to 68% at the intermediate concentration and reaching 90% at the highest concentration investigated. Overall, hydrogen production increased by ~100%. It is to be noted here that the improvement can be attributed to the phenolic compounds, flavonoids and antioxidant constituents present in Bantulsi extract, which enhanced microbial metabolism and stabilized the ZnO nanofluid by minimizing particle aggregation. Consequently, pollutant degradation improved, resulting in higher hydrogen production. Previous literature, for instance, Daglia et al. [39] have also reported that plant-derived polyphenols significantly improve microbial growth and reduce oxidative stress during biological treatment. Additionally, Cushnie and Lamb et al. [44] demonstrated that flavonoids promote microbial metabolic activity and biofilm development, while Devanesan et al. [63] showed that medicinal plant extracts enhanced environmental remediation efficiency by ~30–50% due to their abundant bioactive compounds. Compared with these studies, the present nano-bio-phytochemical system increased hydrogen production from 45% to 90%, demonstrating the effectiveness of Bantulsi extract in enhancing sustainable hydrogen generation.

4. Conclusion

A sustainable nano–bio–phytochemical wastewater treatment strategy was successfully developed by integrating a single-step synthesized ZnO nanofluid, Croton bonplandianum (Bantulsi) extract, and an enriched microbial consortium for simultaneous wastewater remediation and hydrogen production. Molecular characterization confirmed successful enrichment of Enterobacter and Pseudomonas species, exhibiting 97.3–98.8% 16S rRNA sequence identity, 95.93–99.80% BLAST similarity, and an E-value of 0, while the toxicity assessment showed 0 mm zone of inhibition, demonstrating excellent microbial compatibility of the optimized ZnO nanofluid. The developed treatment system substantially improved wastewater quality. Turbidity decreased from 8 NTU to 0 NTU, conductivity from 2103 to 7 µS cm^{-1} (99.67%), TDS from 1280 to 5 mg L^{-1} (99.61%), TSS from 1.1 to 0.008 mg L^{-1} (99.27%), COD from 312 to 5.1 mg L^{-1} (98.37%), and BOD from 46 to 0.8 mg L^{-1} (98.26%), while dissolved oxygen increased from 1.2 to 7.9 mg L^{-1}, indicating efficient restoration of water quality. These values are substantially better than those generally reported for conventional biological, NP-assisted, or phytochemical-based wastewater treatment systems. GC–TCD analysis further demonstrated that the treated wastewater served as an efficient electrolyte for alkaline hydrogen generation. The optimized treatment (S4) achieved ~98% hydrogen production, corresponding to a 112% improvement over untreated wastewater. Parametric optimization revealed that smaller ZnO NPs, an optimum ZnO concentration of 1 wt%, and increasing Bantulsi extract concentration significantly enhanced hydrogen evolution by improving microbial activity, catalytic efficiency, and pollutant degradation.

Overall, this work presents a novel integrated nano–bio–phytochemical platform that combines microbial enrichment, stable ZnO nanofluid technology, and plant-derived phytochemicals within a single treatment process. The excellent purification efficiency, complete

microbial compatibility, and enhanced hydrogen production demonstrate considerable potential for simultaneous wastewater treatment and renewable hydrogen generation. The developed strategy provides a promising route toward circular water management, resource recovery, and sustainable energy production, with strong potential for future pilot-scale implementation and industrial wastewater applications.

Acknowledgments The authors gratefully acknowledge the Council of Science & Technology, Uttar Pradesh, India (CST/E&T/D-1983) for supporting this work. The authors express their sincere gratitude to the Rajiv Gandhi Institute of Petroleum Technology, Jais, for safe conduct of advanced research.

Declarations

Competing interests: The authors declare no competing interests.

Supporting Information: Table S1-S4. Phylogenetic tree of all treated samples.

Data Availability: Data will be made available on request.

References

1. Gleick, P.H.: Basic_Water_Requirements-1996.Pdf, (1996)

2. Falkenmark, M., Rockström, J.: The New Blue and Green Water Paradigm: Breaking New Ground for Water Resources Planning and Management. J. Water Resour. Plan. Manag. 132, 129–132 (2006). https://doi.org/10.1061/(ASCE)0733-9496(2006)132:3(129)

3. Prüss-Ustün, A., Bartram, J., Clasen, T., Colford, J.M., Cumming, O., Curtis, V., Bonjour, S., Dangour, A.D., De France, J., Fewtrell, L., Freeman, M.C., Gordon, B., Hunter, P.R., Johnston, R.B., Mathers, C., Mäusezahl, D., Medlicott, K., Neira, M., Stocks, M., Wolf, J.,

Cairncross, S.: Burden of disease from inadequate water, sanitation and hygiene in low- and middle-income settings: a retrospective analysis of data from 145 countries. Trop. Med. Int. Heal. 19, 894–905 (2014). https://doi.org/10.1111/tmi.12329

4. Macknick, J., Newmark, R., Heath, G., Hallett, K.C.: Operational water consumption and withdrawal factors for electricity generating technologies: a review of existing literature. Environ. Res. Lett. 7, 045802 (2012). https://doi.org/10.1088/1748-9326/7/4/045802

5. Vörösmarty, C.J., McIntyre, P.B., Gessner, M.O., Dudgeon, D., Prusevich, A., Green, P., Glidden, S., Bunn, S.E., Sullivan, C.A., Liermann, C.R., Davies, P.M.: Erratum: Global threats to human water security and river biodiversity. Nature. 468, 334–334 (2010). https://doi.org/10.1038/nature09549

6. Shannon, M.A., Bohn, P.W., Elimelech, M., Georgiadis, J.G., Mariñas, B.J., Mayes, A.M.: Science and technology for water purification in the coming decades. Nature. 452, 301–310 (2008). https://doi.org/10.1038/nature06599

7. Salehi, M.: Global water shortage and potable water safety; Today's concern and tomorrow's crisis. Environ. Int. 158, 106936 (2022). https://doi.org/10.1016/j.envint.2021.106936

8. Rai, P.K.: Impacts of particulate matter pollution on plants: Implications for environmental biomonitoring. Ecotoxicol. Environ. Saf. 129, 120–136 (2016). https://doi.org/10.1016/j.ecoenv.2016.03.012

9. Mekonnen, M.M., Hoekstra, A.Y.: Four billion people facing severe water scarcity. Sci. Adv. 2, 1–7 (2016). https://doi.org/10.1126/sciadv.1500323

10. Sato, T., Qadir, M., Yamamoto, S., Endo, T., Zahoor, A.: Global, regional, and country level

need for data on wastewater generation, treatment, and use. Agric. Water Manag. 130, 1–13 (2013). https://doi.org/10.1016/j.agwat.2013.08.007

11. Oki, T., Kanae, S.: Global Hydrological Cycles and World Water Resources. Science (80-.). 313, 1068–1072 (2006). https://doi.org/10.1126/science.1128845

12. Dahdal, Y.N., Oren, Y., Schwahn, D., Pipich, V., Herzberg, M., Ying, W., Kasher, R., Rapaport, H.: Biopolymer-induced calcium phosphate scaling in membrane-based water treatment systems: Langmuir model films studies. Colloids Surfaces B Biointerfaces. 143, 233–242 (2016). https://doi.org/10.1016/j.colsurfb.2016.02.047

13. Ni, S.Q., Wang, Z., Lv, L., Liang, X., Ren, L., Zhou, Q.: Bioremediation of wastewaters with decabromodiphenyl ether by anaerobic granular sludge. Colloids Surfaces B Biointerfaces. 128, 522–527 (2015). https://doi.org/10.1016/j.colsurfb.2015.03.003

14. Meng, Q., Peng, B., Shen, C.: Synthesis of F127/PAA hydrogels for removal of heavy metal ions from organic wastewater. Colloids Surfaces B Biointerfaces. 167, 176–182 (2018). https://doi.org/10.1016/j.colsurfb.2018.04.024

15. Tchobanoglous, G., L. Burton, F., Stensel, D.H.: Metcalf &Eddy 4th ed., (2014)

16. Jiménez, B., Asano, T.: 2008_Jimenez et al Water reclamation and reuse around the world.

17. Verstraete, W., Van de Caveye, P., Diamantis, V.: Maximum use of resources present in domestic “used water.” Bioresour. Technol. 100, 5537–5545 (2009). https://doi.org/10.1016/j.biortech.2009.05.047

18. Nkwanyana, T.B., Siti, M.W., Wang, Z., Toudjeu, I., Mbungu, N.T., Mulumba, W.: An assessment of hybrid-energy storage systems in the renewable environments. J. Energy

Storage. 72, 108307 (2023). https://doi.org/10.1016/j.est.2023.108307

19. Henze, M.: Characterization of Wastewater for Modelling of Activated Sludge Processes. Water Sci. Technol. 25, 1–15 (1992). https://doi.org/10.2166/wst.1992.0110

20. Stillwell, A.S., King, C.W., Webber, M.E., Duncan, I.J., Hardberger, A.: The Energy-Water Nexus in Texas. Ecol. Soc. 16, art2 (2011). https://doi.org/10.5751/ES-03781-160102

21. Kulikowska, D., Klimiuk, E., Drzewicki, A.: BOD5 and COD removal and sludge production in SBR working with or without anoxic phase. Bioresour. Technol. 98, 1426–1432 (2007). https://doi.org/10.1016/j.biortech.2006.05.021

22. Corominas, L., Foley, J., Guest, J.S., Hospido, A., Larsen, H.F., Morera, S., Shaw, A.: Life cycle assessment applied to wastewater treatment: State of the art. Water Res. 47, 5480–5492 (2013). https://doi.org/10.1016/j.watres.2013.06.049

23. Friedrich, M., Takács, I., Tränckner, J.: Physiological adaptation of growth kinetics in activated sludge. Water Res. 85, 22–30 (2015). https://doi.org/10.1016/j.watres.2015.08.010

24. Liu, Y., Tay, J.-H.: Strategy for minimization of excess sludge production from the activated sludge process. Biotechnol. Adv. 19, 97–107 (2001). https://doi.org/10.1016/S0734-9750(00)00066-5

25. Partow, A.J., Meng, S., Wong, A.J., Savin, D.A., Tong, Z.: Recyclable & highly porous organo-aerogel adsorbents from biowaste for organic contaminants' removal. Sci. Total Environ. 827, 154051 (2022). https://doi.org/10.1016/j.scitotenv.2022.154051

26. Sheng, G.-P., Yu, H.-Q., Li, X.-Y.: Extracellular polymeric substances (EPS) of microbial aggregates in biological wastewater treatment systems: A review. Biotechnol. Adv. 28, 882–

894 (2010). https://doi.org/10.1016/j.biotechadv.2010.08.001

27. Pomiès, M., Choubert, J.-M., Wisniewski, C., Coquery, M.: Modelling of micropollutant removal in biological wastewater treatments: A review. Sci. Total Environ. 443, 733–748 (2013). https://doi.org/10.1016/j.scitotenv.2012.11.037

28. Qu, X., Alvarez, P.J.J., Li, Q.: Applications of nanotechnology in water and wastewater treatment. Water Res. 47, 3931–3946 (2013). https://doi.org/10.1016/j.watres.2012.09.058

29. Wang, J., Ehlig-Economides, C.: Salinity Effect on CO_2 Solubility in Live Formation Water Under Reservoir Conditions. In: SPWLA 64th Annual Symposium Transactions. Society of Petrophysicists and Well Log Analysts (2023)

30. Priya, A.K., Jalil, A.A., Dutta, K., Rajendran, S., Vasseghian, Y., Qin, J., Soto-Moscoso, M.: Microplastics in the environment: Recent developments in characteristic, occurrence, identification and ecological risk. Chemosphere. 298, 134161 (2022). https://doi.org/10.1016/j.chemosphere.2022.134161

31. Lane, D.J., Pace, B., Olsen, G.J., Stahl, D.A., Sogin, M.L., Pace, N.R.: Rapid determination of 16S ribosomal RNA sequences for phylogenetic analyses. Proc. Natl. Acad. Sci. 82, 6955–6959 (1985). https://doi.org/10.1073/pnas.82.20.6955

32. Clarridge, J.E.: Impact of 16S rRNA Gene Sequence Analysis for Identification of Bacteria on Clinical Microbiology and Infectious Diseases. Clin. Microbiol. Rev. 17, 840–862 (2004). https://doi.org/10.1128/CMR.17.4.840-862.2004

33. Janda, J.M., Abbott, S.L.: 16S rRNA Gene Sequencing for Bacterial Identification in the Diagnostic Laboratory: Pluses, Perils, and Pitfalls. J. Clin. Microbiol. 45, 2761–2764 (2007).

https://doi.org/10.1128/JCM.01228-07

34. Brock, T.D., Madigan, M.T., Martinko, J.M.: Biology of microorganisms, Eleventh edition. Biol. Microorg. Elev. Ed. 909 (2006)

35. Davin-Regli, A., Lavigne, J.-P., Pagès, J.-M.: Enterobacter spp.: Update on Taxonomy, Clinical Aspects, and Emerging Antimicrobial Resistance. Clin. Microbiol. Rev. 32, 1–32 (2019). https://doi.org/10.1128/CMR.00002-19

36. Wasi, S., Tabrez, S., Ahmad, M.: Use of Pseudomonas spp. for the bioremediation of environmental pollutants: a review. Environ. Monit. Assess. 185, 8147–8155 (2013). https://doi.org/10.1007/s10661-013-3163-x

37. Pang, Z., Raudonis, R., Glick, B.R., Lin, T.-J., Cheng, Z.: Antibiotic resistance in Pseudomonas aeruginosa: mechanisms and alternative therapeutic strategies. Biotechnol. Adv. 37, 177–192 (2019). https://doi.org/10.1016/j.biotechadv.2018.11.013

38. Sheng, G.P., Yu, H.Q., Li, X.Y.: Extracellular polymeric substances (EPS) of microbial aggregates in biological wastewater treatment systems: A review. Biotechnol. Adv. 28, 882–894 (2010). https://doi.org/10.1016/j.biotechadv.2010.08.001

39. Daglia, M.: Polyphenols as antimicrobial agents. Curr. Opin. Biotechnol. 23, 174–181 (2012). https://doi.org/10.1016/j.copbio.2011.08.007

40. Jain, K., Patel, A.S., Pardhi, V.P., Flora, S.J.S.: Nanotechnology in Wastewater Management: A New Paradigm Towards Wastewater Treatment. Molecules. 26, 1797 (2021). https://doi.org/10.3390/molecules26061797

41. Raghupathi, K.R., Koodali, R.T., Manna, A.C.: Size-dependent bacterial growth inhibition

and mechanism of antibacterial activity of zinc oxide nanoparticles. Langmuir. 27, 4020–4028 (2011). https://doi.org/10.1021/la104825u

42. Sirelkhatim, A., Mahmud, S., Seeni, A., Kaus, N.H.M., Ann, L.C., Bakhori, S.K.M., Hasan, H., Mohamad, D.: Review on Zinc Oxide Nanoparticles: Antibacterial Activity and Toxicity Mechanism. Nano-Micro Lett. 7, 219–242 (2015). https://doi.org/10.1007/s40820-015-0040-x

43. Zhang, D.Q., Eng, C.Y., Stuckey, D.C., Zhou, Y.: Effects of ZnO nanoparticle exposure on wastewater treatment and soluble microbial products (SMPs) in an anoxic-aerobic membrane bioreactor. Chemosphere. 171, 446–459 (2017). https://doi.org/10.1016/j.chemosphere.2016.12.053

44. Cushnie, T.P.T., Lamb, A.J.: Recent advances in understanding the antibacterial properties of flavonoids. Int. J. Antimicrob. Agents. 38, 99–107 (2011). https://doi.org/10.1016/j.ijantimicag.2011.02.014

45. Cushnie, T.P.T., Lamb, A.J.: Errata for "Antimicrobial activity of flavonoids" [Int. J. Antimicrob. Agents 26 (2005) 343–356]. Int. J. Antimicrob. Agents. 27, 181 (2006). https://doi.org/10.1016/j.ijantimicag.2005.12.002

46. Glick, B.R.: Plant Growth-Promoting Bacteria: Mechanisms and Applications. Scientifica (Cairo). 2012, 1–15 (2012). https://doi.org/10.6064/2012/963401

47. Jia, Y.H., Choi, J.Y., Ryu, J.H., Kim, C.H., Lee, W.K., Tran, H.T., Zhang, R.H., Ahn, D.H.: Hydrogen production from wastewater using a microbial electrolysis cell. Korean J. Chem. Eng. 27, 1854–1859 (2010). https://doi.org/10.1007/s11814-010-0310-8

48. Bhattacharjee, S.: DLS and zeta potential – What they are and what they are not? J. Control. Release. 235, 337–351 (2016). https://doi.org/10.1016/j.jconrel.2016.06.017

49. Avogadro, C.: Israelachvili_2011_Intermolecular-Surface-Forces_3rd-ed.

50. Srivastava, R., Chaturvedi, K.R., Sharma, T., Hirani, H., Tripathi, N.M.: Stable TiO_2 – Surfactant Hybrid System for Improving Foam Stability and Mobility Control: Experimental and Mechanistic Insights. Energy & Fuels. (2026). https://doi.org/10.1021/acs.energyfuels.6c01450

51. Srivastava, R., Yadav, M.K., Sharma, T., Hirani, H., Velmurugan, N.: Performance of a Stable Hybrid TiO_2 /SiO_2 Nanocomposite in the Thermophysical Characterization of Organic PCM (Stearic Acid) for Thermal Energy Storage. ACS Appl. Energy Mater. (2026). https://doi.org/10.1021/acsaem.6c00967

52. Hembram, B.K., Srivastava, R., Sharma, T., Prasad, S.K.: Influence of single-step synthesized SiO_2 nanofluids on formation kinetics and storage capacity of CO_2 hydrate. J. Indian Chem. Soc. 103, 102764 (2026). https://doi.org/10.1016/j.jics.2026.102764

53. Yadav, M.K., Srivastava, R., Sharma, T., Trivedi, J.: Impact of single-step nanofluid of independent particle size and controllable properties on thermal energy storage potential of organic PCM. Chem. Pap. (2026). https://doi.org/10.1007/s11696-026-05311-5

54. Harborne, J.B.: Phytochemical methods. In: A guide to modern techniques of plant analysis. (1973)

55. del Castillo, A.F., Garibay, M.V., Díaz-Vázquez, D., Yebra-Montes, C., Brown, L.E., Johnson, A., Garcia-Gonzalez, A., Gradilla-Hernández, M.S.: Improving river water quality

prediction with hybrid machine learning and temporal analysis. Ecol. Inform. 82, 102655 (2024). https://doi.org/10.1016/j.ecoinf.2024.102655

56. Guide for Ultra-Pure Water Used in the Electronics and Semiconductor Industries, http://www.astm.org/cgi-bin/resolver.cgi?D5127-13R18, (2018)

57. Tombs, M.C.: John C. Crittenden, R. Rhodes Trussell, David W. Hand, Kerry J. Howe, George Tchobanoglous: MWH Water Treatment Principles and Design. Third Edition. Chromatographia. 77, 527–528 (2014). https://doi.org/10.1007/s10337-013-2600-x

58. Basak, B.B., Saha, A., Sarkar, B., Kumar, B.P., Gajbhiye, N.A., Banerjee, A.: Repurposing distillation waste biomass and low-value mineral resources through biochar-mineral-complex for sustainable production of high-value medicinal plants and soil quality improvement. Sci. Total Environ. 760, 143319 (2021). https://doi.org/10.1016/j.scitotenv.2020.143319

59. Manisha, M., Verma, K., Ramesh, N., Anirudha, T.P., Santrupt, R.M., Rao, L.: Water, sanitation, and hygiene implications of large-scale recycling of treated municipal wastewater in semi-arid regions. Sci. Total Environ. 904, 166631 (2023). https://doi.org/10.1016/j.scitotenv.2023.166631

60. Chang, J. Sen, Chong, M.N., Poh, P.E., Ocon, J.D., Md Zoqratt, M.Z.H., Lee, S.M.: Impacts of morphological-controlled ZnO nanoarchitectures on aerobic microbial communities during real wastewater treatment in an aerobic-photocatalytic system. Environ. Pollut. 259, 113867 (2020). https://doi.org/10.1016/j.envpol.2019.113867

61. Zang, W., Sharma, R., Li, M.W.H., Fan, X.: Retention Time Trajectory Matching for Peak Identification in Chromatographic Analysis. Sensors. 23, 1–18 (2023).

https://doi.org/10.3390/s23136029

62. Raghupathi, K.R., Koodali, R.T., Manna, A.C.: Size-Dependent Bacterial Growth Inhibition and Mechanism of Antibacterial Activity of Zinc Oxide Nanoparticles. Langmuir. 27, 4020–4028 (2011). https://doi.org/10.1021/la104825u

63. Devanesan, S., AlSalhi, M.S., Asemi, N.N., AlNatheer, Y., Shanmuganathan, R., Brindhadevi, K.: Deciphering the fluorescence quenching potential of Croton bonplandianum leaves and detection of bioactive molecules using liquid chromatography and mass spectrometry. Chemosphere. 319, 138024 (2023). https://doi.org/10.1016/j.chemosphere.2023.138024

Tables:

Table 1 Composition of all 4 Petri plates used to grow microbes, detailing the volume of agar, ZnO nanofluid, extract, and activated sludge.

Sample name	Agar Conc.	ZnO Nanofluid	Bio extract	STP (activated sludge)
S1	2ml	_	_	2ml
S2	2ml	1ml	_	1ml
S3	2ml	_	1ml	1ml
S4	3ml	1ml	1ml	1ml

Table 2 Parameters of Raw STP water sample compared to Ultra-Pure Water (UPW), including TDS, Conductivity, and BOD.

Parameter	Unit	Wastewater (Outlet)	Ultra-Pure Water
Turbidity	NTU	8 to 9	< 0.05
Total Dissolved Solids (TDS)	mg/L (ppm)	500 – 1500	0 – 1

Total Suspended Solids (TSS)	mg/L	<30	~ 0
Conductivity	µS/cm	1800 – 2200	0.055
Dissolved Oxygen (DO)	mg/L	1.2 – 2.2	8 – 9
Biochemical Oxygen Demand (BOD)	mg/L	< 30	0
Chemical Oxygen Demand (COD)	mg/L	< 200	0

Table 3 Dynamic Light Scattering (DLS) data for ZnO nanofluid.

Precursor	Accelerator	Particle size (nm)	Zeta potential (mV)	Concentration (Weight %)
Zinc acetate dihydrate	Ammonium hydroxide			
2.2 mg	5 mL	21	-48	1 wt%

Table 4 Final physicochemical parameters (Turbidity, TDS, Suspended Solids, DO, and Conductivity) for treated samples (S1-S4)

Sample name	Turbidity (NTU)	TDS (ppm)	TSS (mg/L)	DO (mg/L)	Conductivity (µS/cm)
S1	0.5	22	1.1	5.2	27
S2	0	13	0.1	6.7	16
S3	0	11	0.15	7.8	12
S4	0	5	0.008	7.9	7

Figures:

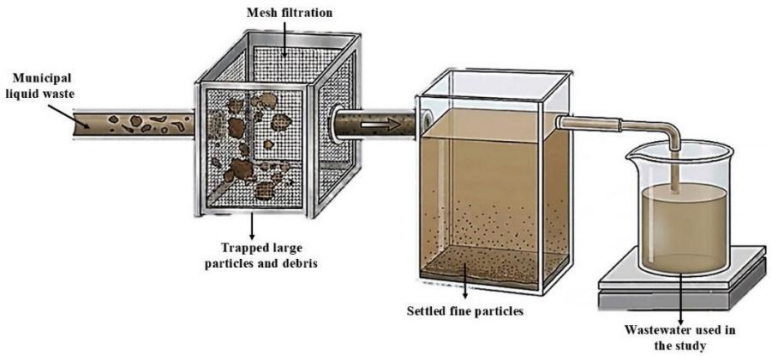

Fig. 1 Schematic representation of wastewater collection, mesh filtration (100 µm), sedimentation, and separation of supernatant wastewater for subsequent treatment.

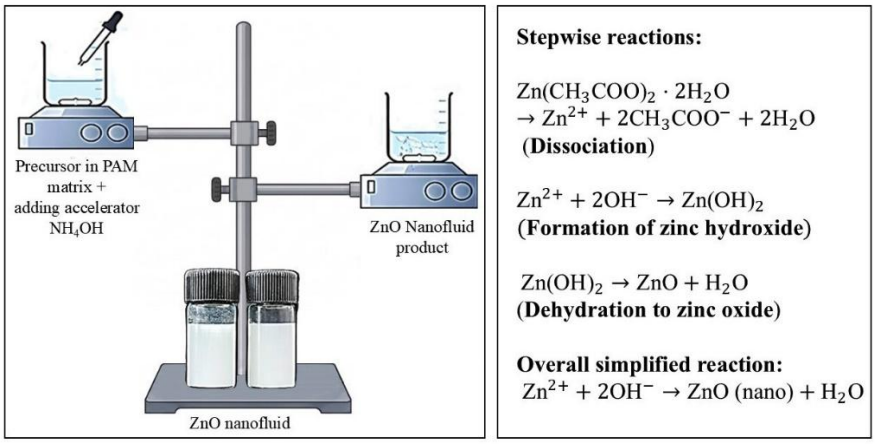

Fig. 2 Schematic illustration of ZnO nanofluid synthesis through the sol–gel route using zinc acetate dihydrate, ammonium hydroxide, and PAM as a stabilizing agent. (With reactions involved)

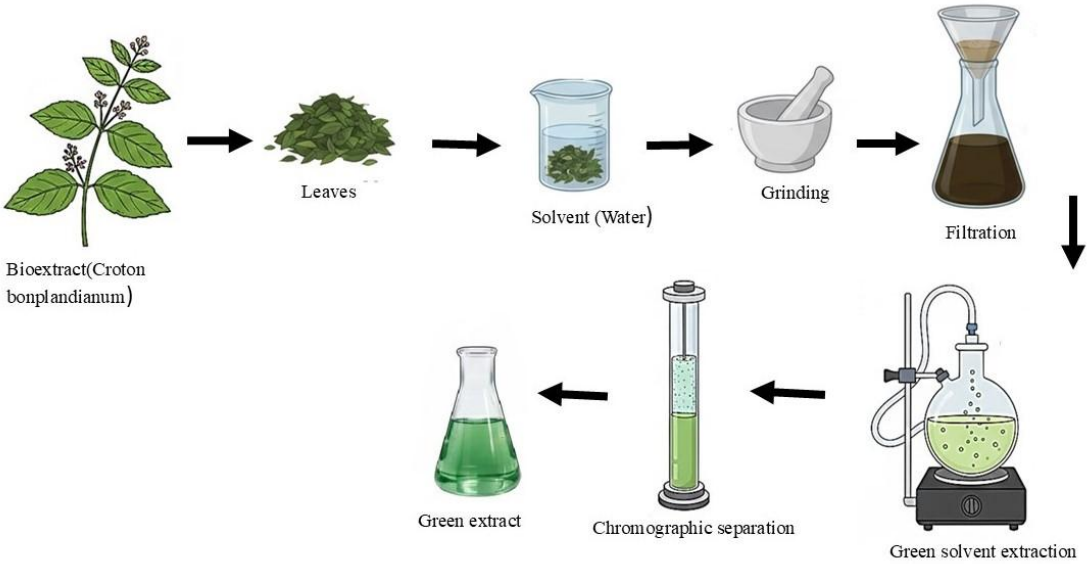

Fig. 3 Preparation of *Croton bonplandianum* leaf extract through washing, crushing, aqueous extraction, heating, and filtration steps.

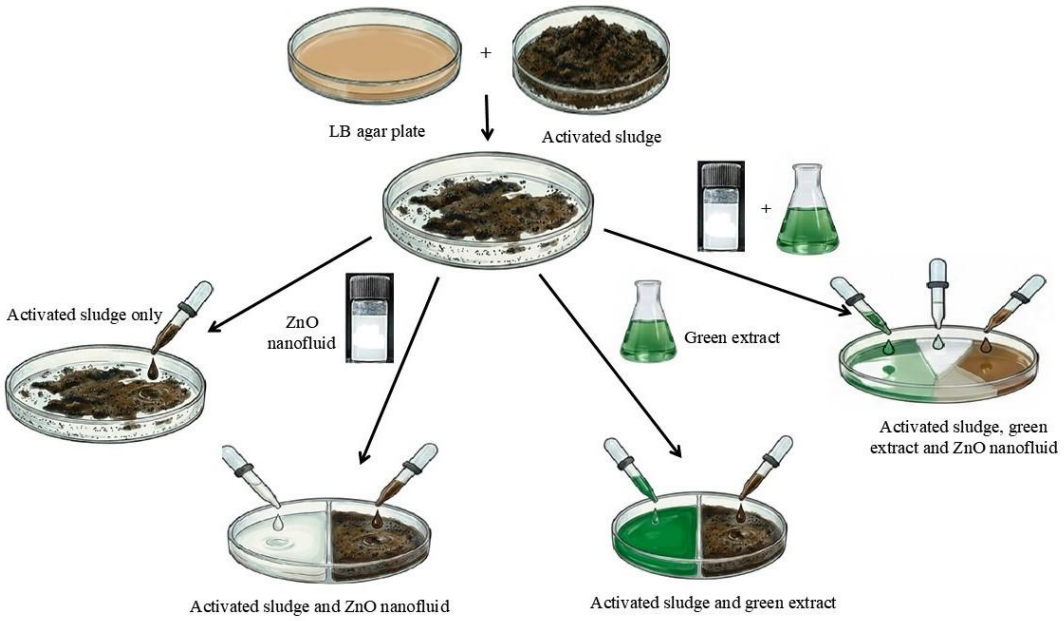

Fig. 4A Schematic representation of microbial enrichment using activated sludge in the presence of ZnO nanofluid and plant-derived phytochemicals prior to wastewater treatment.

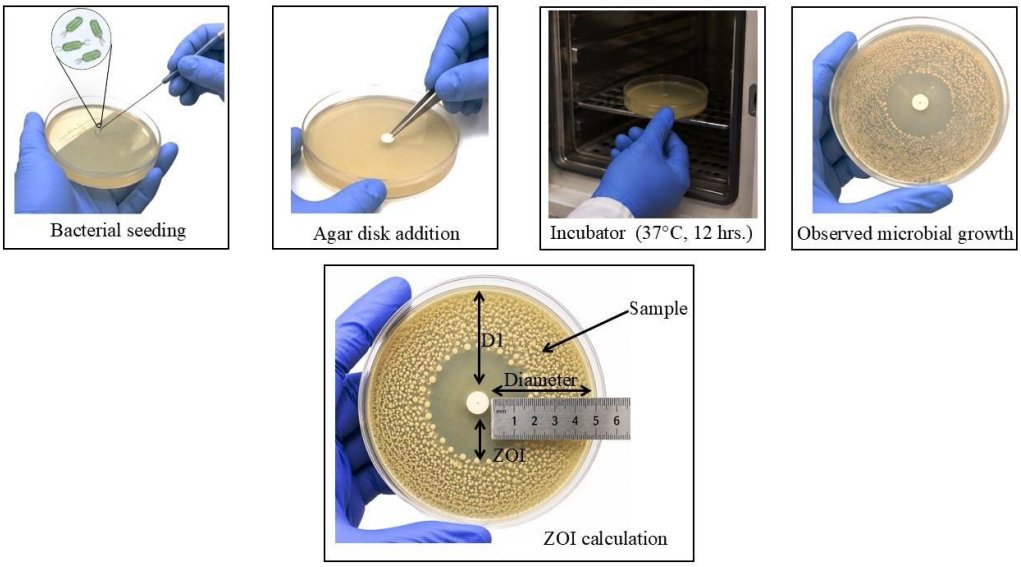

Fig. 4B Schematic representation of microbial toxicity assessment using the agar well diffusion method for determining ZOI.

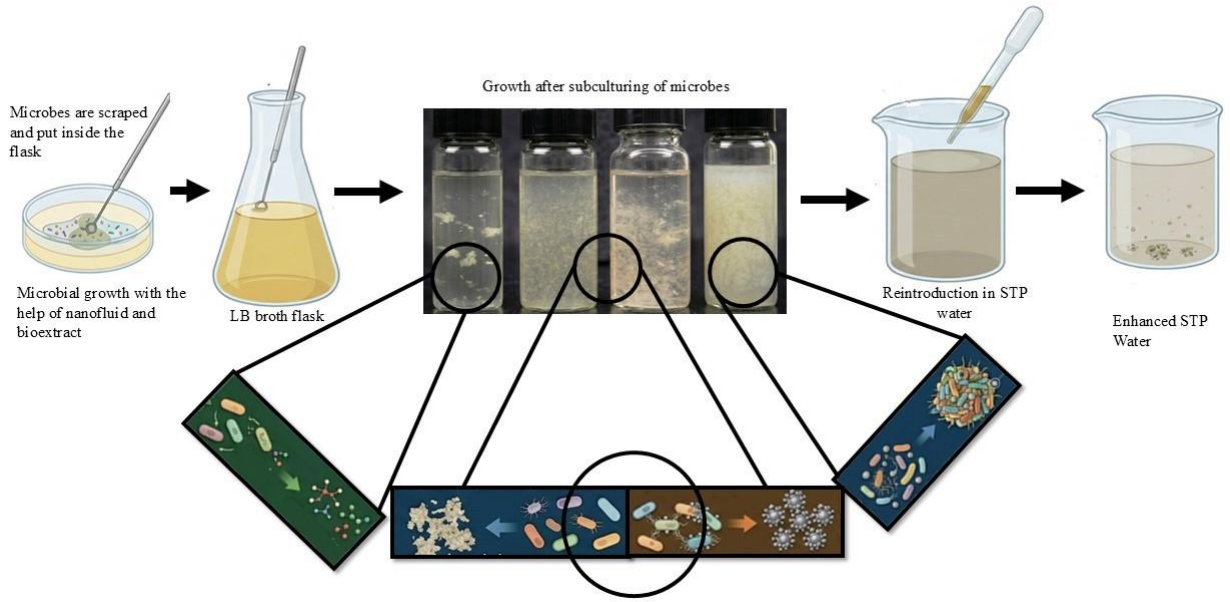

Fig. 5A Experimental workflow showing LB agar preparation, microbial enrichment on agar plates, bulk cultivation in LB broth, and subsequent inoculation of wastewater samples.

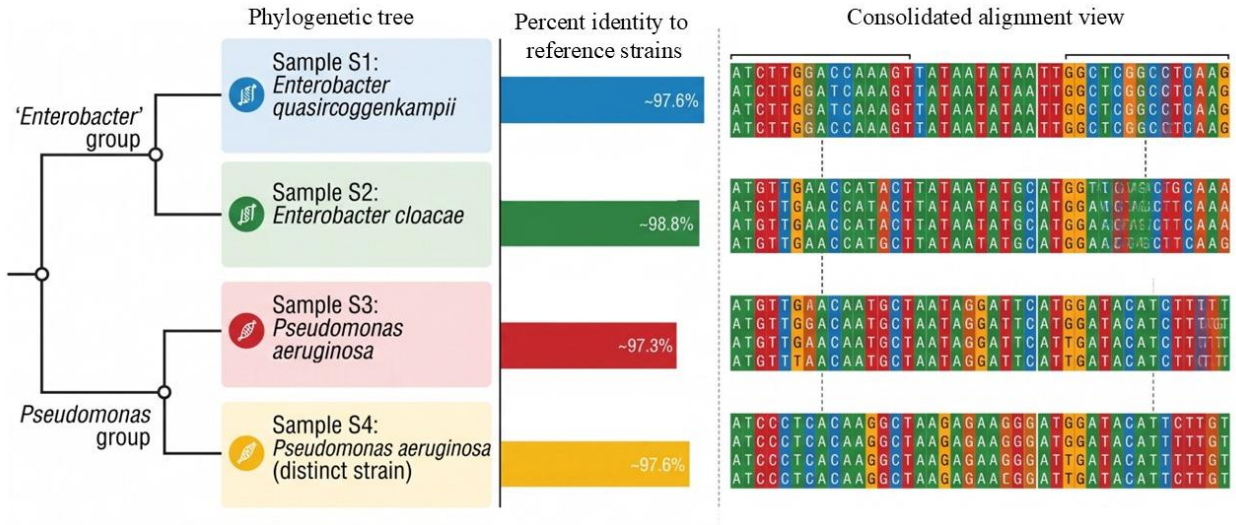

Fig. 5B Phylogenetic and sequence alignment analysis of microbial samples. *(Left)* Phylogenetic tree showing the evolutionary relationships and percent sequence identities of isolated samples (S1–S4) relative to reference strains *(Right)* illustrating isolated bacterial strains.

Percentage majority identification score											
Sample S1:Enterobacter quasiroggenkampii			Sample S2: Enterobacter cloacae			Sample S3: Pseudomonas aeruginosa			Sample S4: Pseudomonas aeruginosa		
	BLAST Hit Description	% Majority Identification Score		BLAST Hit Description	% Majority Identification Score		BLAST Hit Description	% Majority Identification Score		BLAST Hit Description	% Majority Identification Score
1	*Enterobacter quasiroggenkampii* (NR_179166.1)	96.69%	1	*Enterobacter cloacae* (NR_117679.1)	98.94%	1	*Pseudomonas aeruginosa* (NR_117678.1)	99.80%	1	*Pseudomonas aeruginosa* (NR_117678.1)	95.93%
2	*Enterobacter mori* (NR_146667.2)	97.62%	2	*Enterobacter cloacae* subsp. *dissolvens* (NR_118011.1)	98.88%	2	*Pseudomonas aeruginosa* (NR_114471.1)	99.73%	2	*Pseudomonas aeruginosa* (NR_113599.1)	95.93%
3	*Enterobacter sichuanensis* (NR_179946.1)	97.43%	3	*Enterobacter cloacae* (NR_102794.2)	98.68%	3	*Pseudomonas aeruginosa* (NR_113599.1)	99.79%	3	*Pseudomonas aeruginosa* (NR_114471.1)	95.93%
4	*E. chengduensis* (NR_146667.2)	97.62%	4	*E. cloacae cloacae* (NR_117679.1)	98.68%	4	*Metapseudomonas otitidis* (NR_117678.1)	99.80%	4	*Metapseudomonas otitidis* (NR_117678.1)	95.93%
5	*E. wuhouensis* (NR_146667.2)	97.62%	5	*E. cloacae cloacae* (NR_117679.1)	98.68%	5	*P. tohonis* (NR_113599.1)	99.73%	5	*Metapseudomonas otitidis* (NR_113599.1)	95.93%
6	*E. chuandaensis* (NR_179946.1)	97.43%	6	*E. cloacae cloacae* (NR_117679.1)	98.68%	6	*P. tohonis* (NR_117678.1)	99.73%	6	*Metapseudomonas lalkuanensis*	95.93%
8	*E. ludwigii* (NR_146667.2)	97.43%	8	*Pseudenterobacter* (NR_102794.2)	98.68%	8	*P. aeruginosa* DSM 50071 (NR_113599.1)	99.79%	8	*Pseudomonas guezennei*	95.93%
9	*E. ludwigii* (NR_179166.1)	97.43%	9	*Pseudenterobacter timonensis* (NR-I521)	98.68%	9	*Metapseudomonas otitidis* (NR_113599.1)	99.79%	9	*Pseudomonas*	95.93%
10	*Leclercia adecarboxylata* (NR_179166.1)	96.69%	10	*Leclercia adecarboxylata* (NR_102794.2)	98.68%	10	*P. aeruginosa* DSM 50071 (NR_113599.1)	99.79%	10	*Metapseudomonas phytobenefica*	95.93%
12	*Pantoea agglomerans*	97.62%	10	*Enterobacter chengduensis*	98.68%	12	*Metapseudomonas* species	99.80%	12	*Pseudomonas aeruginosa* DSM 50071	95.93%

Fig. 5C BLAST identification and percent similarity scores for isolates S1–S4. Tabular summary with corresponding percentage majority identification scores for samples S1-S4.

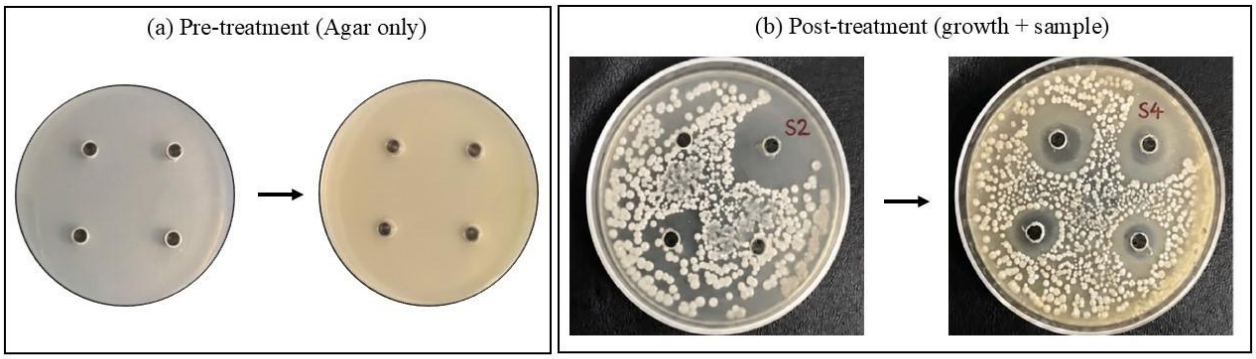

Sample	Pre-treatment (control)	Post-treatment	Mean ZOI (mm)	Biocompatibility assessment
S2	Agar only	Growth + S2	0	Non-toxic
S4	Agar only	Growth + S4	0	Non-toxic

Fig. 5D Toxicity evaluation via agar diffusion assay**.** *(Top)* Plate images illustrating agar wells pre-treatment (agar only) and post-treatment (microbial growth with sample introduction) for S2 and S4. *(Bottom)* Summary table detailing the mean zone of inhibition (ZOI = 0 mm) and resulting biocompatibility assessments, demonstrating non-toxic characteristics.

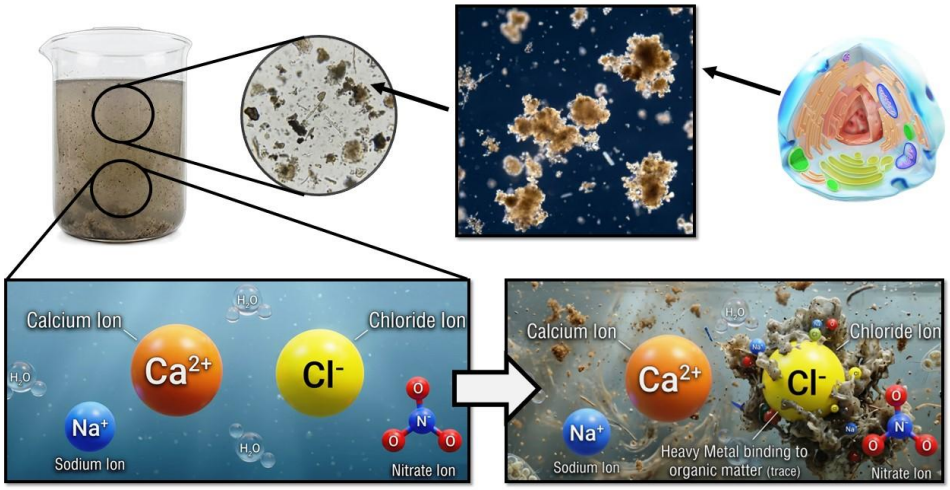

Fig. 6 Visual representation of wastewater showing high organic, ionic load and microbial contaminants (as proposed at the bottom side in the Fig.).

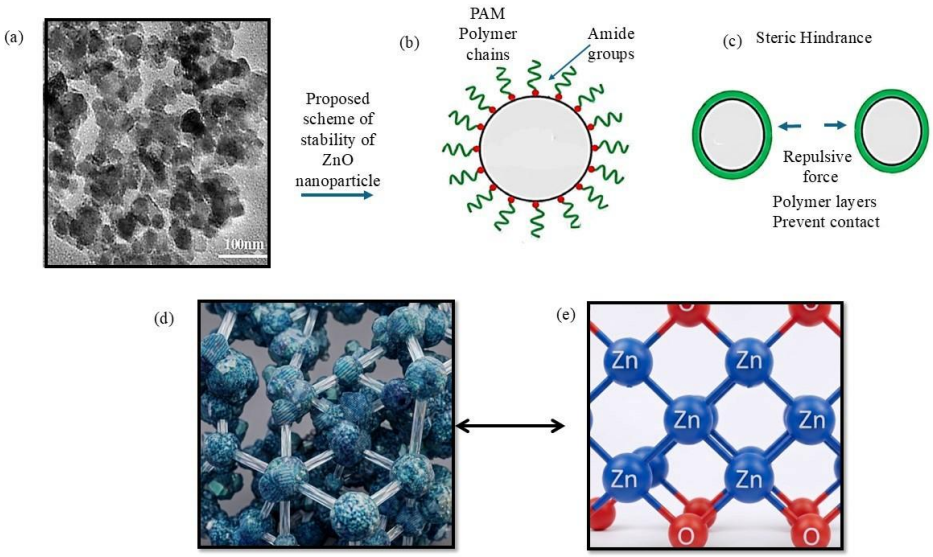

Fig. 7 TEM characterization of ZnO–PAM nanofluid: (a) TEM image showing the overall dispersion of ZnO NPs; (b) proposed stability scheme of ZnO NPs; (c) steric stabilization of ZnO NPs; (d) enlarged view illustrating the interparticle spacing and uniform NP distribution within the PAM matrix; and (e) proposed steric stabilization mechanism of ZnO NPs by PAM.

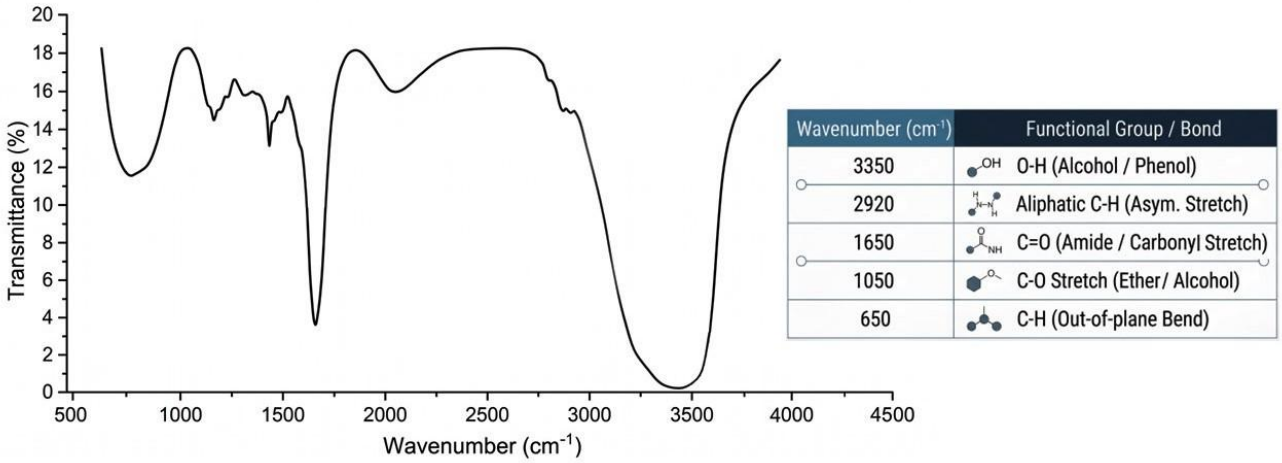

Fig. 8 FTIR spectrum of *Croton bonplandianum* extract showing characteristic O–H, C–H, C=O, and C–O functional groups associated with phenolic and flavonoid phytochemicals.

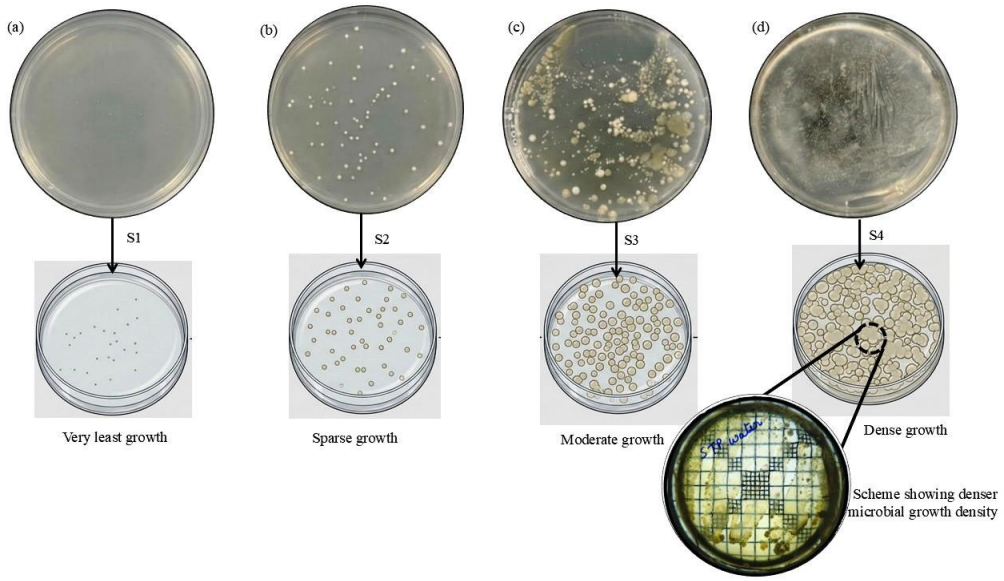

Fig. 9 Microbial colony growth on LB agar plates under different enrichment conditions: (a) S1 (activated sludge), (b) S2 (activated sludge + ZnO nanofluid), (c) S3 (activated sludge + plant extract), and (d) S4 (activated sludge + ZnO nanofluid + plant extract).

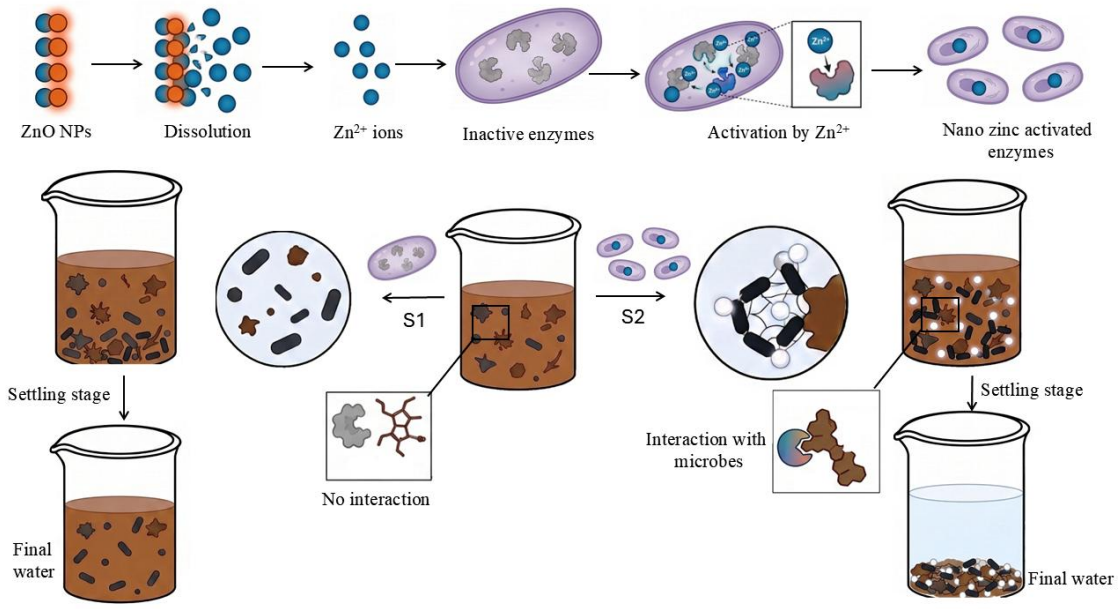

Fig. 10A Proposed mechanism of turbidity and TSS reduction through microbial degradation and ZnO nanoparticle-assisted bio flocculation. ZnO nanoparticles enhance enzymatic activity, promote aggregation of suspended particles, and facilitate formation and settling of larger bioflocs.

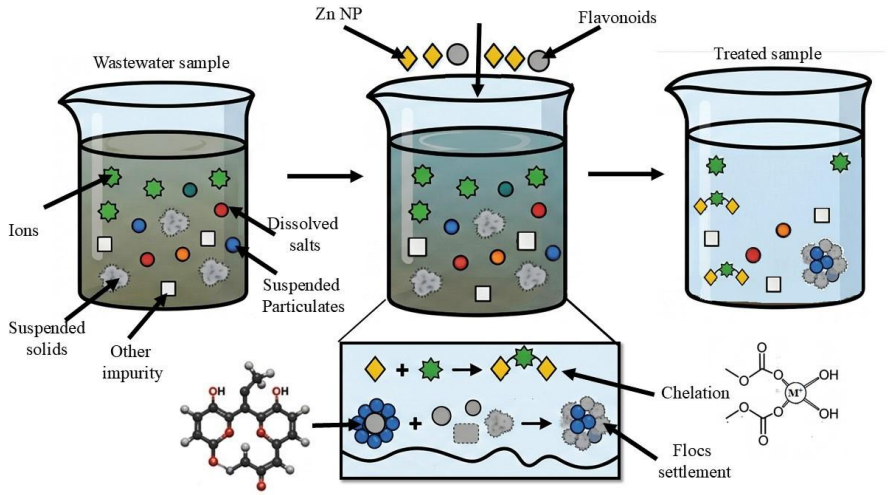

Fig. 10B Proposed mechanism of phytochemical-assisted pollutant removal. Flavonoids and phenolic compounds present in *Croton* extract promote microbial metabolism, contaminant complexation, and aggregation of organic particles through chelation and molecular interactions.

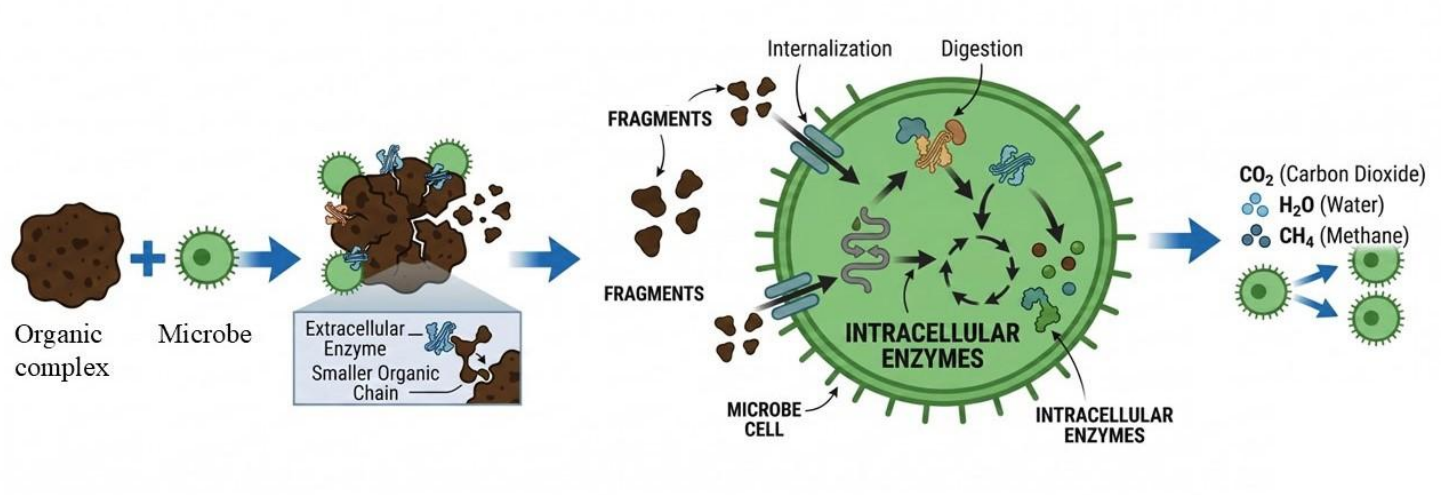

Fig. 10C Proposed synergistic nano–bio–phytochemical treatment mechanism showing the combined action of ZnO nanofluid, plant-derived phytochemicals, and enriched microbial communities.

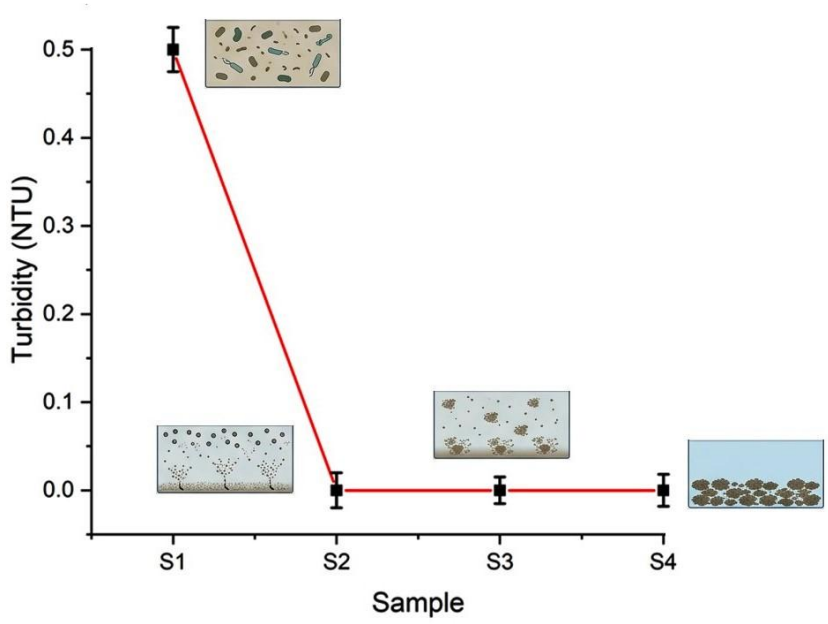

Fig. 11 Variation in turbidity of wastewater samples treated with S1–S4 microbial consortia showing progressive reduction in suspended and colloidal matter.

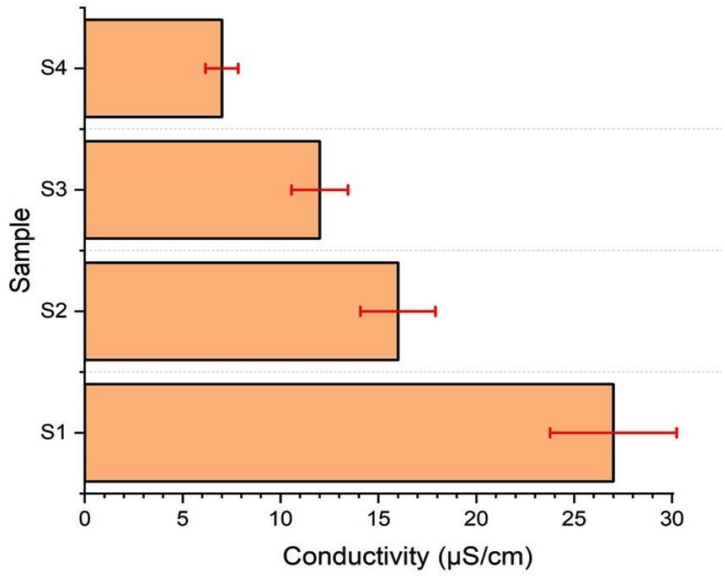

Fig. 12 Conductivity of untreated wastewater and treated samples (S1–S4), illustrating progressive removal of dissolved ionic contaminants during treatment.

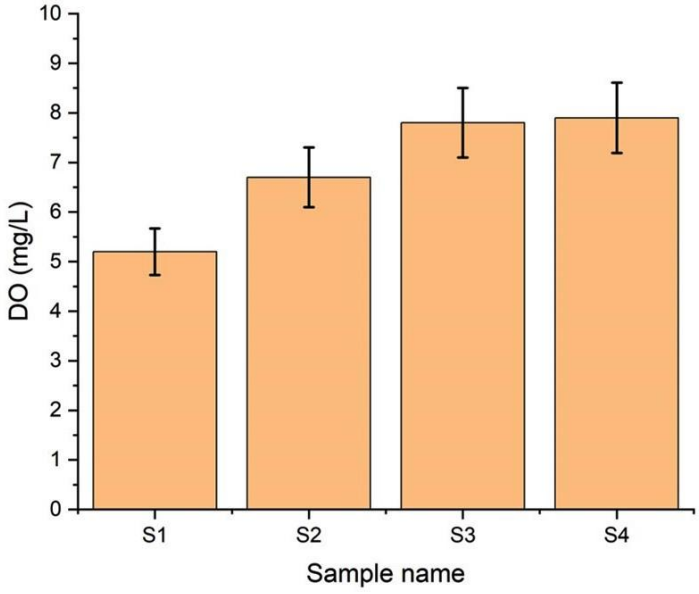

Fig. 13 DO concentration of untreated wastewater and treated samples (S1–S4), demonstrating improved oxygen availability following pollutant degradation.

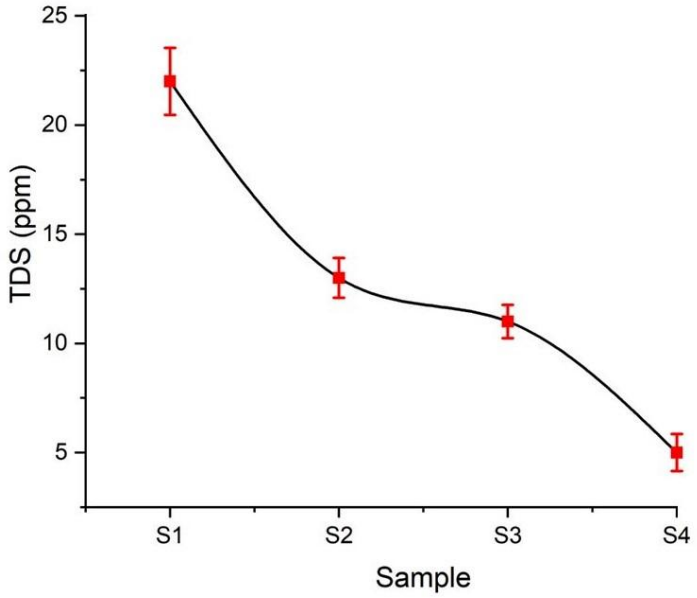

Fig. 14 TDS concentration of untreated wastewater and treated samples (S1–S4), showing reduction of dissolved contaminants through the nano–bio–phytochemical treatment process.

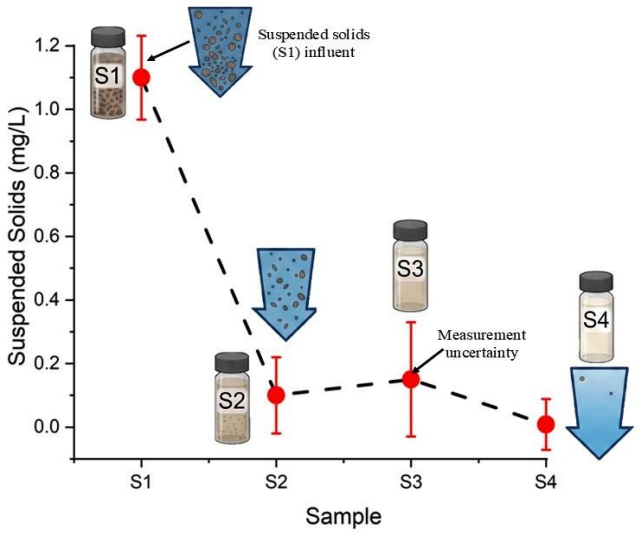

Fig. 15 TSS of treated wastewater samples (S1–S4), demonstrating enhanced particulate removal and biofloc settling efficiency.

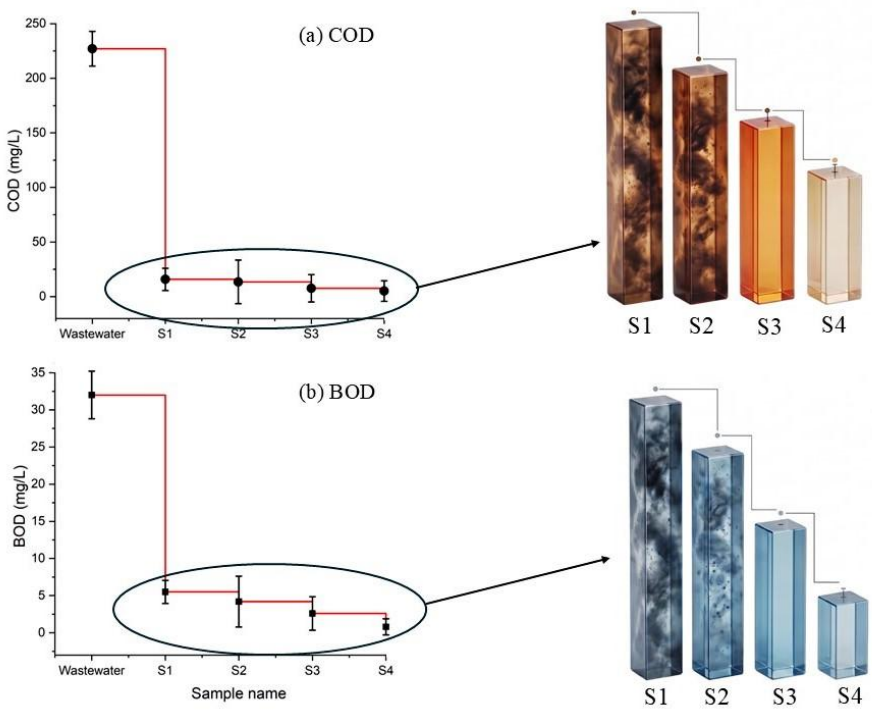

Fig. 16 Changes in organic pollution indicators following treatment: (a) Chemical oxygen demand (COD) and (b) Biochemical oxygen demand (BOD) of untreated wastewater and treated samples (S1–S4), showing progressive degradation and mineralization of organic contaminants.

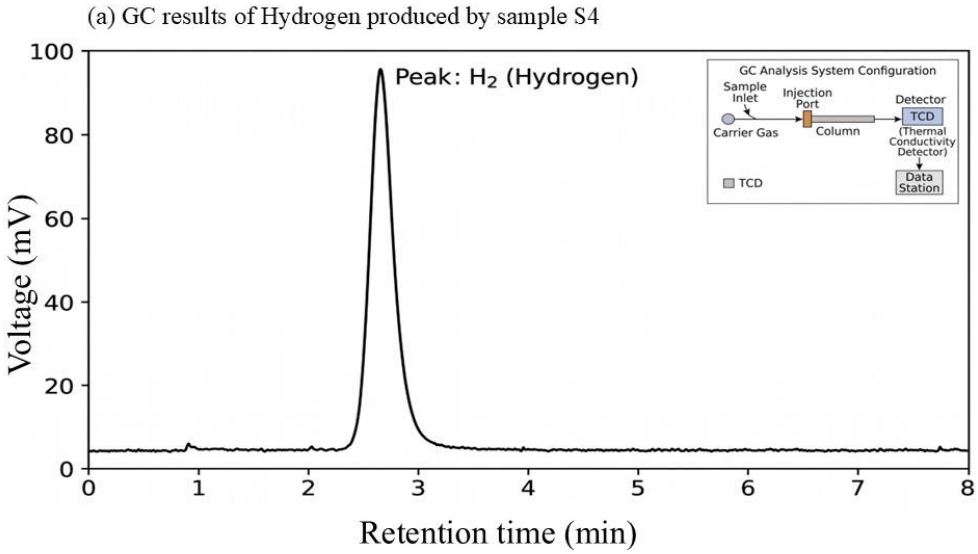

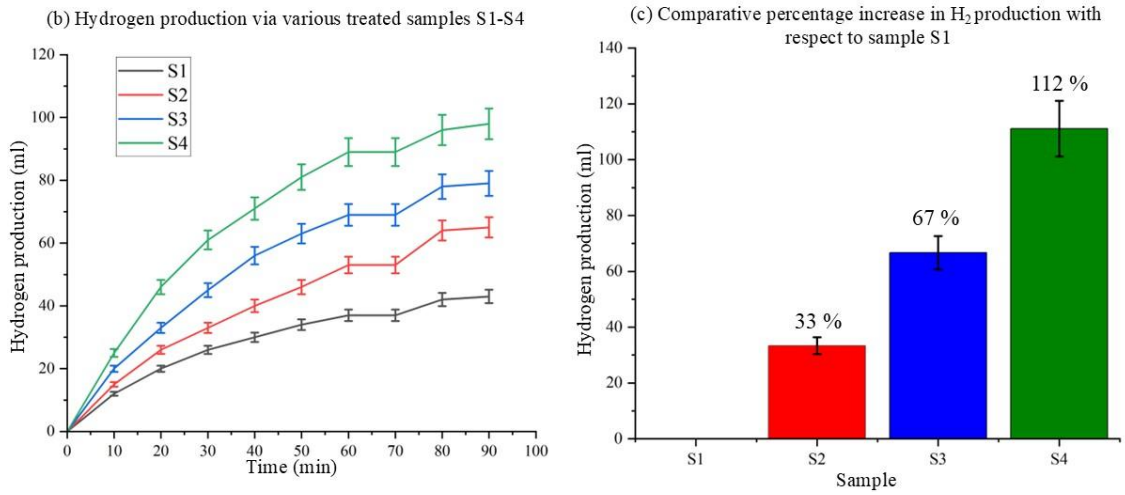

Fig. 17 Gas chromatographic analysis and comparative hydrogen production performance. (a) Representative GC spectrum highlighting the detected hydrogen peak; (b) Cumulative hydrogen production volume over time (0–90 min) for treated samples S1 through S4; and (c) Percentage increase in total H_2 yield for samples S2, S3, and S4 relative to the baseline sample S1.

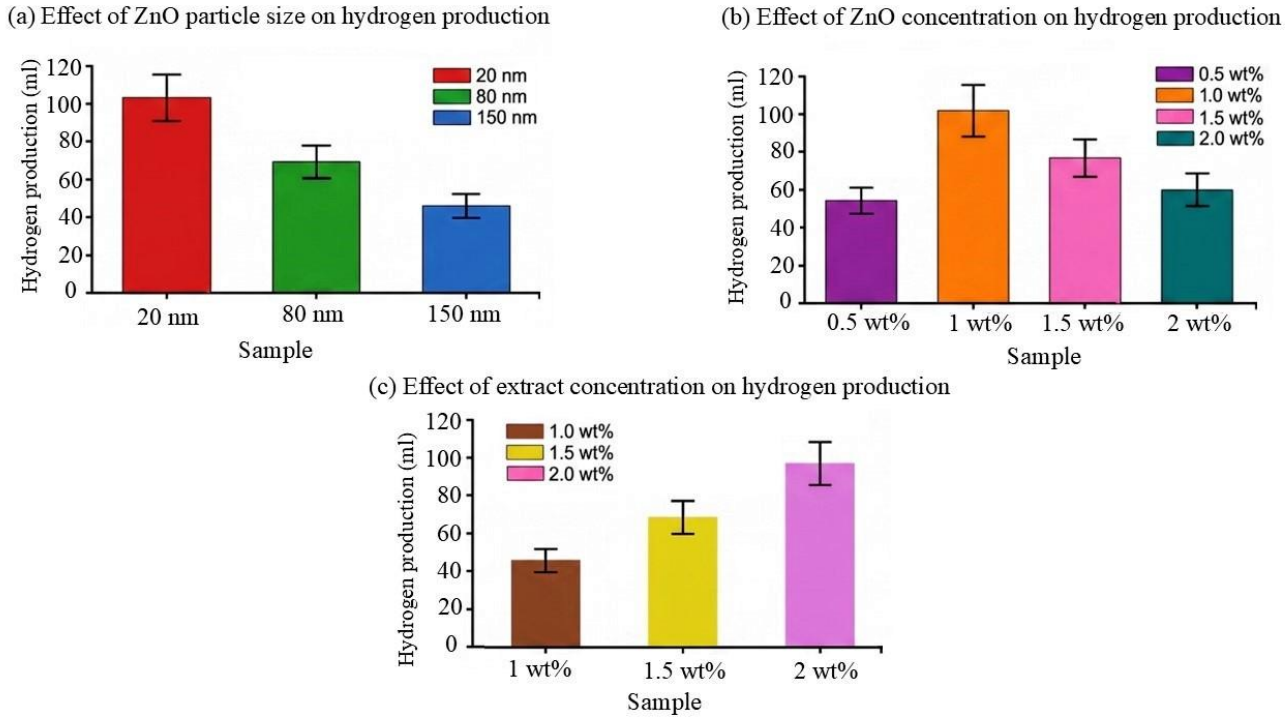

Fig. 18 Parametric effects on microbial hydrogen production. (a) Influence of ZnO NP size; (b) Effect of ZnO NP concentration; and (c) Effect of plant extract concentration on H_2 generation.

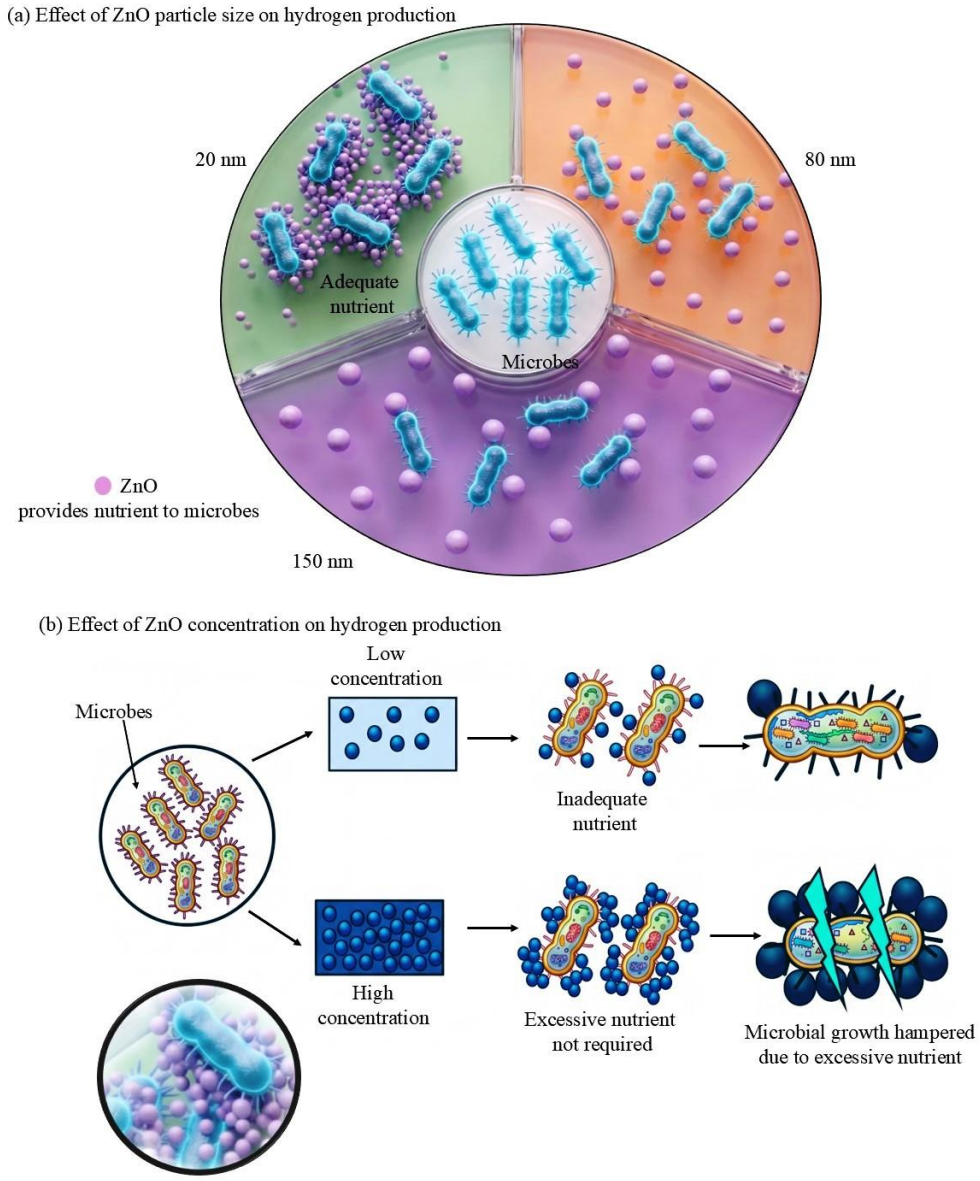

Fig. 19 Proposed mechanism for the effects of ZnO NP size and concentration on microbial activity. (a) Schematic showing the interaction of different ZnO particle sizes; and (b) illustrating the concentration-dependent response: low concentrations, and excessive concentrations inhibit microbial metabolism due to cellular.

Supplementary Files

This is a list of supplementary files associated with this preprint. Click to download.

- StatementofNovelty.docx